A3: Effective field theories for threshold states

B8: heavy quarkonium

Yu Jia

IHEP

The 7th Symposium on "Symmetries and the emergence of Structure in QCD", Rizhao, ShanDong, July 19-July 22, 2023

A3 and B8 in the third term

PI: Nora Brambilla, Y.J., Antonio Vairo

External collaborators (Chinese side):

Feng Feng (China University of Mining and Technology, Beijing)

Wen-Long Sang (Southwest University, ChongQing)

Representative Work of A3 on Chinese side

1) Y. S. Huang, F. Feng, **Y. J**, W. L. Sang, D. S. Yang and J. Y. Zhang, Inclusive production of fully-charmed 1^{+-} tetraquark at B factory, Chin. Phys. C 45, no. 9, 093101 (2021)

2) F. Feng, Y. S. Huang, **Y. J.**, W. L. Sang and J. Y. Zhang, Exclusive radiative production of fully-charmed tetraquarks at B factor, Phys. Lett. B 818, 136368 (2021)

3) F. Feng, Y. S. Huang, **Y. J.**, W. L. Sang, X.N. Xiong and J. Y. Zhang, Fragmentation production of fully-charmed tetraquarks at the LHC, Phys. Rev. D 106, no. 11, 114029 (2022)

4) F. Feng, Y. Huang, **Y. J.**, W. L. Sang, D. S. Yang and J. Y. Zhang, Inclusive production of fully-charmed tetraquarks at LHC. [arXiv:2304.11142 [hep-ph]].

Representative Work of B8 on Chinese side

1) W. L. Sang, F. Feng, **Y. Jia**, Z. Mo, J. Pan and J. Y. Zhang, Optimized $\mathcal{O}({\alpha_s}^2)$ correction to exclusive double J/φ production at B factories. [arXiv:2306.11538 [hep-ph]].

2) W. L. Sang, F. Feng, **Y. Jia**, Z. Mo and J. Y. Zhang, $\mathcal{O}({\alpha_s}^2)$ corrections to $J/\varphi + \chi_{c0,1,2}$ production at B factories, Phys. Lett. B 843, 138057. (2023)

3) **Y. Jia**, Z. W. Mo, J. C. Pan, and J. Y. Zhang, Photoproduction of C-even quarkonia at EIC and EicC. To appear in PRD. [arXiv:2207.14171 [hep-ph]].

4) F. Feng, **Y. Jia**, Z. Mo, J. Pan, W. L. Sang and J. Y. Zhang, Complete three-loop QCD corrections to leptonic width of vector quarkonium. [arXiv:2207.14259 [hep-ph]].

5) F. Feng, **Y. Jia**, Z. W. Mo, J. C. Pan and W. L. Sang , Three-loop QCD corrections to the decay constant of B_c. [arXiv:2208.04302 [hep-ph]].

6)F. Feng, **Y. Jia**, Z. Mo, W. L. Sang and J. Y. Zhang, Next-to-next-to-leading-order QCD corrections to $e^+e^- \to J/\varphi + \eta_c$ at B factories. [arXiv:1901.08447 [hep-ph]]

Develop NRQCD factorization formalism to decribe the production of fully-charmed tetraquark

(Unexpected) discovery of X(6900) in summer of 2020

Invariant mass spectrum of J/ψ-pair candidates (LHCb, 2020)

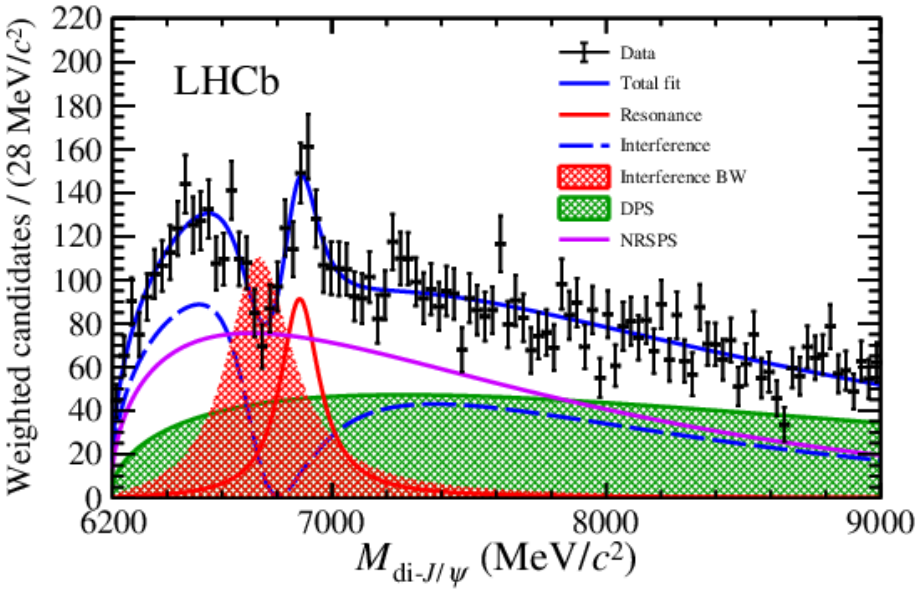

LHCb discovered a narrow structure near 6.9 GeV in the di-J/ψ invariant mass spectrum:X(6900).

Strong candidate for compact fully-charmed tetraquark

There' s also a board structure above threshold ranging from 6.2 to 6.8 GeV

An additional vague structure near 7.2 GeV

See W.-L. Sang's talk in this symposium

Interpretation of nature of the X(6900) meson

- **P-wave tetraquark** (M.-S. Liu et al., 2020; H.-X. Chen et al., 2020, R. Zhu 2020).
- **Radial excitation of 0++** (Z.-G. Wang, 2020; Lü et al., 2020; Giron, Lebed, 2020; Karliner & Rosner, 2020; J. Zhao et al., 2020; R. Zhu, 2020; B.-C. Yang et al., 2020; Z. Zhao, 2020; H.-W. Ke et al., 2020),
- **Ground state S-wave tetraquark** (Gordillo et al., 2020).
- $\chi_{c0}\chi_{c0}$ **or** $p_c p_c$ **molecular state** (Albuquerque et al., 2020)
- 0^{++} **hybrid** (B.-D. Wan, C.-F. Qiao, 2020),
- **Resonance formed in charmonium-charmonium scattering** (G. Yang et al., 2020; X. Jin et al., 2020), or the kinematic cusp arising from final-state interaction(J.-Z.Wang et al., 2020; X.-K. Dong et al., 2020; Z.-H. Guo 2021; C. Gong et al. 2020).
- **Beyond Standard Model scenario** (J.-W. Zhu et al., 2020; Dosch et al., 2020)

Popular phenomenological tools handling fully-heavy tetraquark

Theoretical explorations on fully heavy tetraquarks date back to 1970s

Iwasaki, PRL(1976); Chao, ZPC(1981); Ader et al. PRD(1982)

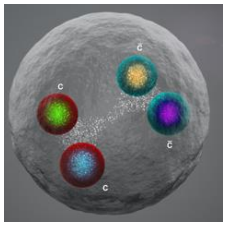

- **Potential models** studying T4c spectra and decay properties: (Badalian et al., 1987; Barnea et al., 2006; Liu et al., 2019; Wu et al., 2018), etc.

- **QCD sum rule**: (H.-X. Chen et al., 2020; W. Chen et al., 2017, 2018; Wang, 2017, 2020; Wang & Di, 2019)

- Search for the fully-bottom tetraquark on **Lattice NRQCD**: found no indication of any states below $2\eta_b$ threshold in the 0^{++},1^{+-} and 2^{++} channels (Hugheset al., 2018).

T4c production mechanisms in the market

- In contrast to mass spectra and decay channels, there is relatively sparse studies for T_{4c} production in various enviorment.

- **Duality relation** model: comparing di-J/psi production cross section with (Berezhnoy et al., 2011; Berezhnoy et al., 2012) and without resonance, rough estimate was achieved (Karliner et al., 2017)
- Treat hadronization within **color evaporation model:** (Carvalho et al., 2016; Maciuła et al., 2020)

- **NRQCD-inspired factorization**: F. Feng, Y.-S. Huang, Y.J, W.-L.Sang, X.-N. Xiong, J.-Y. Zhang and D.-S. Yang, 2020-2023

Also see Y.-Q. Ma, Zhang, 2020; R.-L. Zhu, 2020.

- γγ interactions: Gonçalves, Moreira, 2021.

Nonrelativistic QCD (NRQCD): Paradigm of EFT, tailored for describing heavy quarkonium dynamics: exploiting NR nature of quarkonium

Caswell, Lepage (1986); Bodwin, Braaten, Lepage (1995)

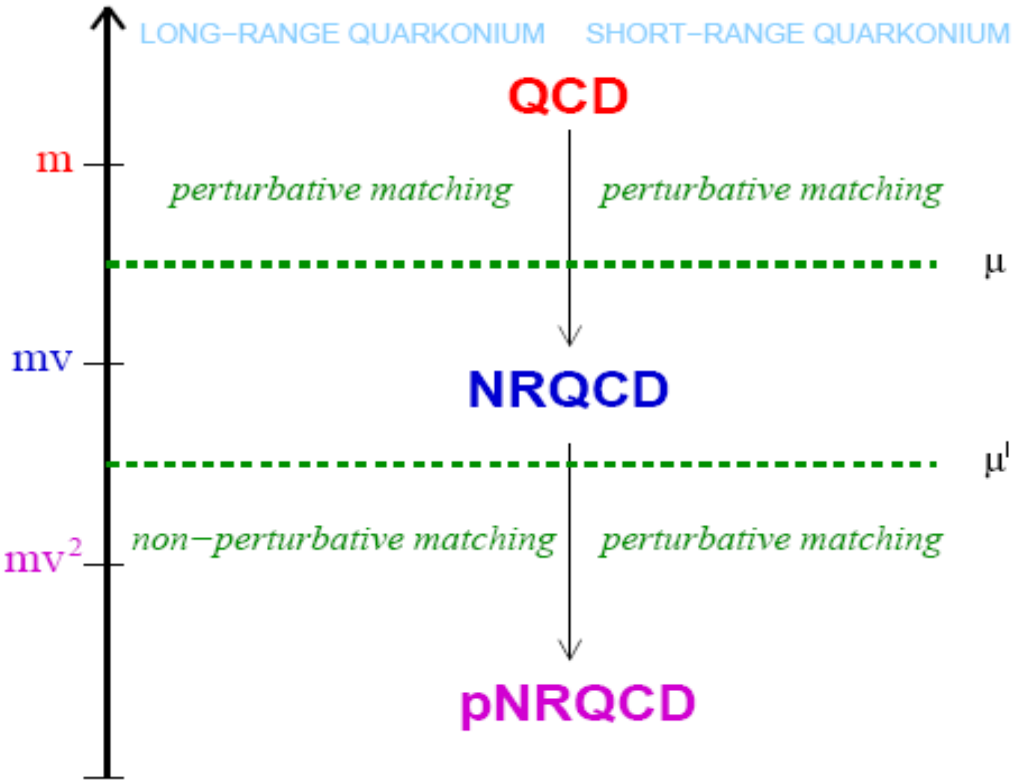

NRQCD factorization is viewed as being first principle of QCD

This scale separation is usually referred to as **NRQCD factorization.**

The NRQCD short-dist. coefficients can be computed in perturbation theory, order by order

QCD Factorization Theorem

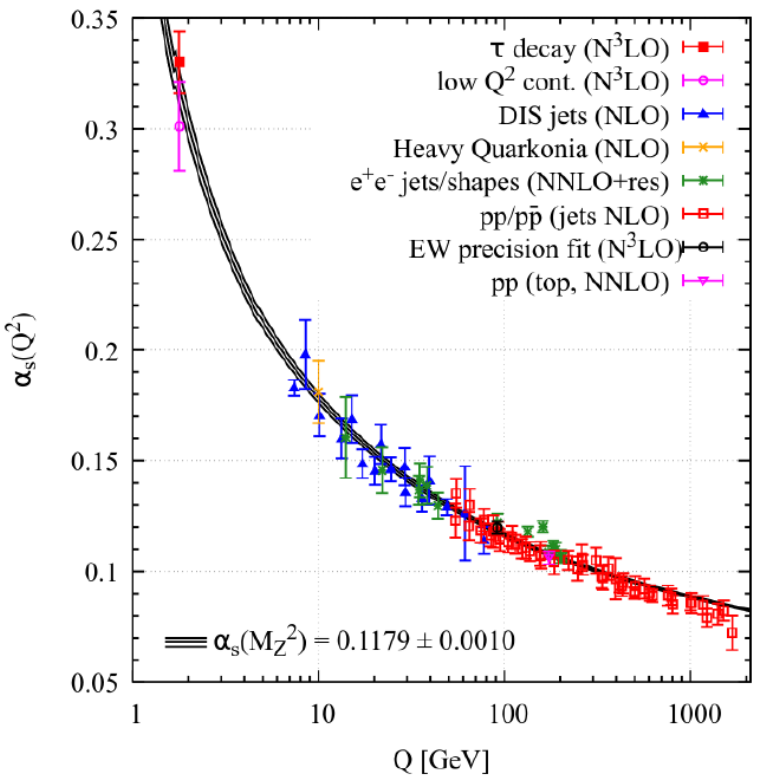

- Asymptotic freedom
- Scale separation: UV ~ Q (pT for production), IR~ Λ_{QCD}
- QCD Collinear factorization theorem:

$$\sigma(Q, \Lambda_{\mathrm{QCD}}) = \hat{\sigma}_{\mathrm{pert}}(Q, \mu_F) \otimes \varphi(\mu_F, \Lambda_{\mathrm{QCD}}) + \cdots$$

- This allows perturbative calculation to produce sensible phenomenological results

QCD factorization theorem for the identified hadron inclusive production at large P_T

Collins, Soper, Sterman (1982)

$$d\sigma[A+B\to H(P_\perp)+X]=\sum_i d\hat{\sigma}[A+B\to i(P_\perp/z)+X]\otimes D_{i\to H}(z,\mu)+\mathcal{O}(1/P_\perp^2)$$

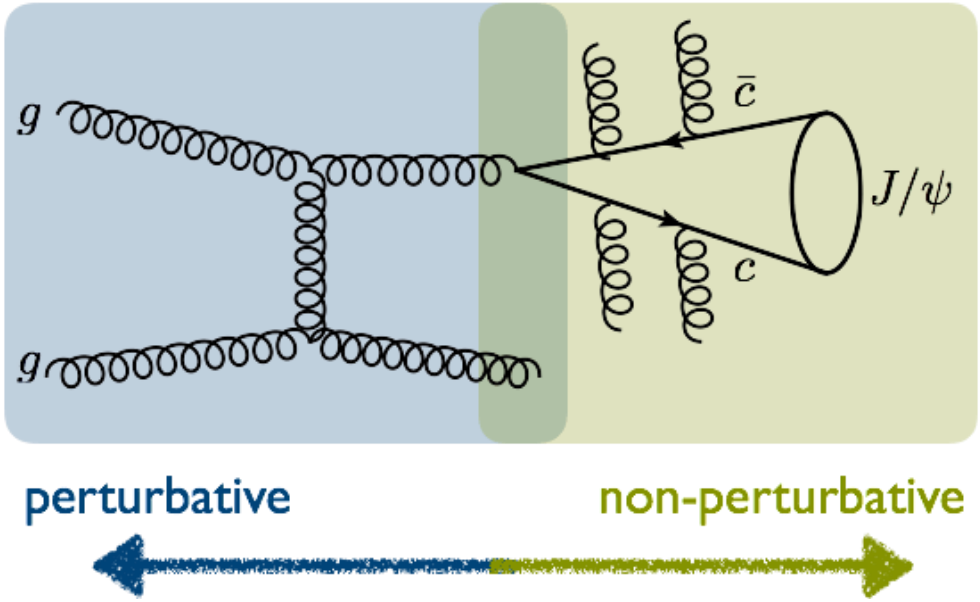

The inclusive production of high-transverse-momentum hadrons in the high-energy hadron collision experiments is dominated by the fragmentation mechanism.

Feynman Diagrams for the fragmentation function of gluon into fully-heavy tetraquark

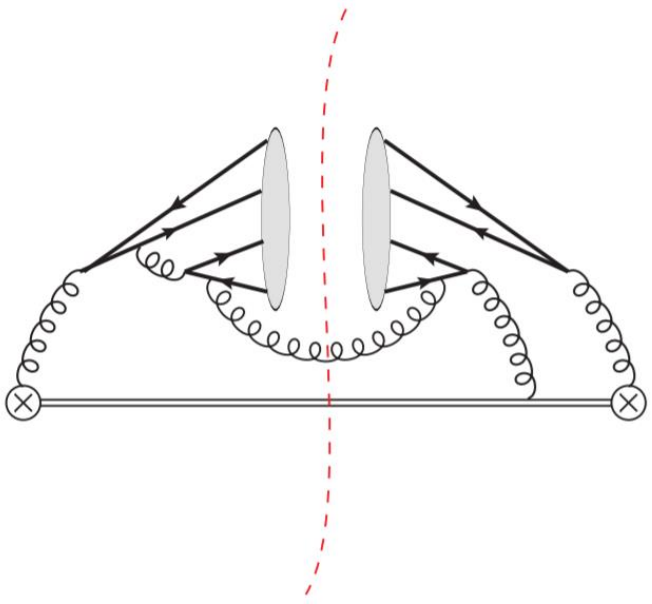

About 100 diagrams for amplitude in one side of the cut line

Key insight: to create a T_{4c} state, one has to first produce four charm quarks with small velocity before hadronization. Therefore, one can invoke perturbation theory to compute the hard partonic process owing to asymptotic freedom of QCD

NRQCD Factorization for the gluon-to-0^{++} (2^{++}) T4c fragmentation function

For the gluon-to-tetraquark fragmentation function:

$$D_{g\to T_{4c}}(z,\mu_\Lambda) = \frac{d_{3,3}\left[g\to cc\bar{c}\bar{c}^{(J)}\right]}{m^9}\left|\left\langle 0\left|\mathcal{O}^{(J)}_{\mathbf{3}\otimes\bar{\mathbf{3}}}\right|T^{(J)}_{4c}\right\rangle\right|^2 + \frac{d_{6,6}\left[g\to cc\bar{c}\bar{c}^{(J)}\right]}{m^9}\left|\left\langle 0\left|\mathcal{O}^{(J)}_{\mathbf{6}\otimes\bar{\mathbf{6}}}\right|T^{(J)}_{4c}\right\rangle\right|^2$$
$$+\frac{d_{3,6}\left[g\to cc\bar{c}\bar{c}^{(J)}\right]}{m^9}2\mathrm{Re}\left[\left\langle 0\left|\mathcal{O}^{(J)}_{\mathbf{3}\otimes\bar{\mathbf{3}}}\right|T^{(J)}_{4c}\right\rangle\left\langle T^{(J)}_{4c}\left|\mathcal{O}^{(J)\dagger}_{\mathbf{6}\otimes\bar{\mathbf{6}}}\right|0\right\rangle\right]+\cdots,$$

Lowest order in v;
Vacuum saturation approximation invoked

S-wave NRQCD production operators (using diquark-antidiquark color-spin basis)

We construct the NRQCD local operators for the S-wave tetraquark with all possible quantum numbers:

$$O^{(0)}_{\bar{\mathbf{3}}\otimes\mathbf{3}} = -\frac{1}{\sqrt{3}}[\psi_a^\dagger \sigma^i (i\sigma^2)\psi_b^*][\chi_c^T (i\sigma^2)\sigma^i \chi_d]\, C^{ab;cd}_{\bar{\mathbf{3}}\otimes\mathbf{3}},$$

$$O^{(0)}_{\mathbf{6}\otimes\bar{\mathbf{6}}} = \frac{1}{\sqrt{6}}[\psi_a^\dagger (i\sigma^2)\psi_b^*][\chi_c^T (i\sigma^2)\chi_d]\, C^{ab;cd}_{\mathbf{6}\otimes\bar{\mathbf{6}}},$$

$$O^{(2)kl}_{\bar{\mathbf{3}}\otimes\mathbf{3}} = [\psi_a^\dagger \sigma^m (i\sigma^2)\psi_b^*][\chi_c^T (i\sigma^2)\sigma^n \chi_d]\, \Gamma^{kl;mn}\, C^{ab;cd}_{\bar{\mathbf{3}}\otimes\mathbf{3}},$$

$$\mathcal{O}^i_{\bar{\mathbf{3}}\otimes\mathbf{3}} = \frac{1}{\sqrt{2}}\epsilon^{ijk} C^{ab;cd}_{\bar{\mathbf{3}}\otimes\mathbf{3}} \left(\psi_a^\dagger \sigma^j i\sigma^2 \psi_b^*\right)\left(\chi_c^T i\sigma^2 \sigma^k \chi_d\right)$$

$$C^{ab;cd}_{\mathbf{3}\otimes\bar{\mathbf{3}}} \equiv \frac{1}{(\sqrt{2})^2}\epsilon^{abm}\epsilon^{cdn}\frac{\delta^{mn}}{\sqrt{3}} = \frac{1}{2\sqrt{N_c}}(\delta^{ac}\delta^{bd} - \delta^{ad}\delta^{bc})$$

$$C^{ab;cd}_{\bar{\mathbf{6}}\otimes\mathbf{6}} \equiv \frac{1}{2\sqrt{6}}(\delta^{ac}\delta^{bd} + \delta^{ad}\delta^{bc}). \quad \Gamma^{kl;mn} \equiv \frac{1}{2}(\delta^{km}\delta^{ln} + \delta^{kn}\delta^{lm} - \frac{2}{3}\delta^{kl}\delta^{mn})$$

Determine short-distance coefficients (SDC) through *perturbative matching*

The SDCs are state-independent quantities, insensitive to non-perturbative (long-distance) physics

Use free quark states instead of hadron (tetraquark) state in both FF and LDMEs

Perturbatively calculate both FF and LDMEs; solve the matching equation and deduce the SDCs

Adopt angular momentum eigenstates and project perturbative FF to specific color state in order to deduce each SDCs in question

Estimation of Long-Distance Matrix Elements (LDMEs) from potential models

- The NRQCD LDMEs should be calculated in lattice QCD in principle since they are non-perturbative.
- We use three phenomenological four-quark models tocalculate the LDMEs. The results are proportional to thewave functions at the origin.

$$\langle T^J_{4c} | O^J_{\text{color}} | 0 \rangle_{\text{I}} = \frac{1}{\pi^2}\sqrt{\frac{105}{2}} R^J_{\text{I, color}}(0)$$

$$\langle T^J_{4c} | O^J_{\text{color}} | 0 \rangle_{\text{II}} = 4\psi^J_{\text{color}}(0)$$

$$\langle T^J_{4c} | O^J_{\text{color}} | 0 \rangle_{\text{III}} = \frac{1}{2\pi^{3/2}} R^J_{\text{III, color}}(0)$$

- The numerical values are: (GeV$^{9/2}$)

Model	Ref.	$\langle T^0_{4c} \lvert O^{(0)}_{\bar{\mathbf{3}}\otimes\mathbf{3}} \rvert 0 \rangle$	$\langle T^0_{4c} \lvert O^{(0)}_{\mathbf{6}\otimes\bar{\mathbf{6}}} \rvert 0 \rangle$	$\langle T^2_{4c} \lvert O^{(2)}_{\bar{\mathbf{3}}\otimes\mathbf{3}} \rvert 0 \rangle$
I	Zhao et al., 2020	2.402	2.085	1.865
II	Lü et al., 2020	−0.1864	−0.1132	0.1200
III	Liu et al., 2020	−0.136737	0.117944	0.112084

Evolution of Fragmentation Function under DGLAP

- Since the process is gluon dominance, the leading order splitting kernels read (nf: number of active light quark flavors):

$$P_{g\leftarrow g}(z) = 6\left[\frac{(1-z)}{z} + \frac{z}{(1-z)_+} + z(1-z) + \left(\frac{11}{12} - \frac{n_{\rm f}}{18}\right)\delta(1-z)\right]$$

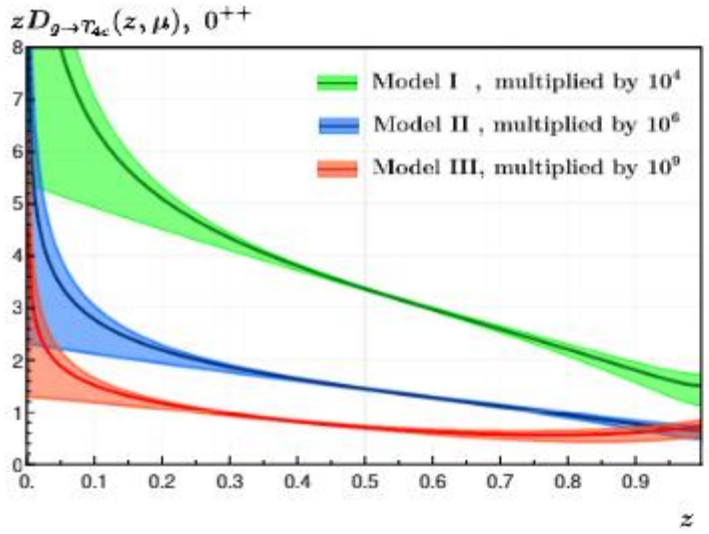

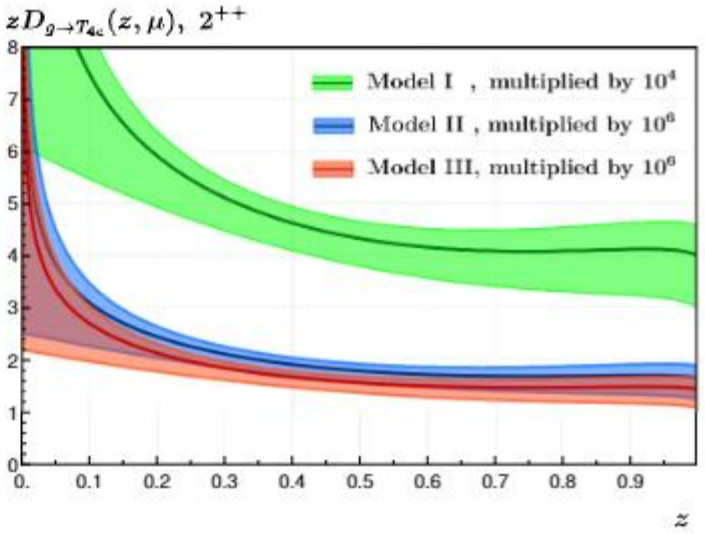

Phenomenology at LHC

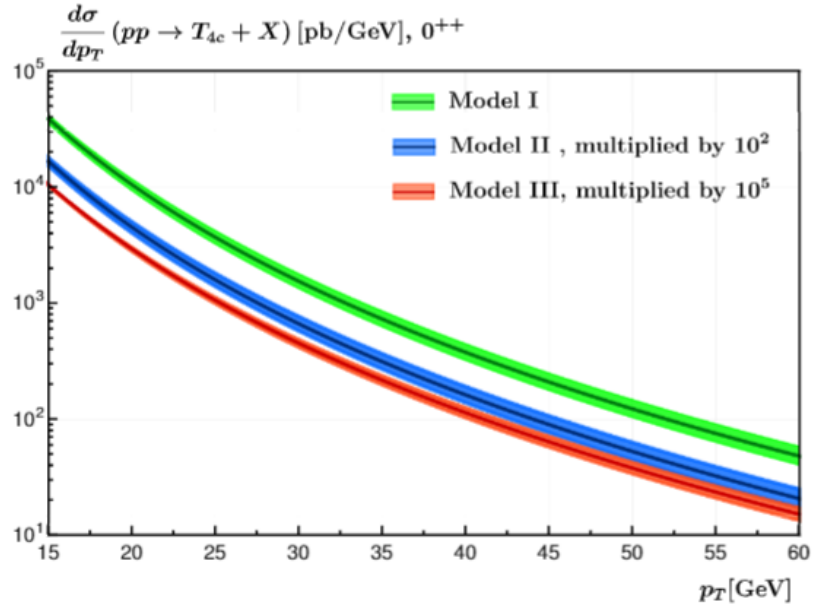

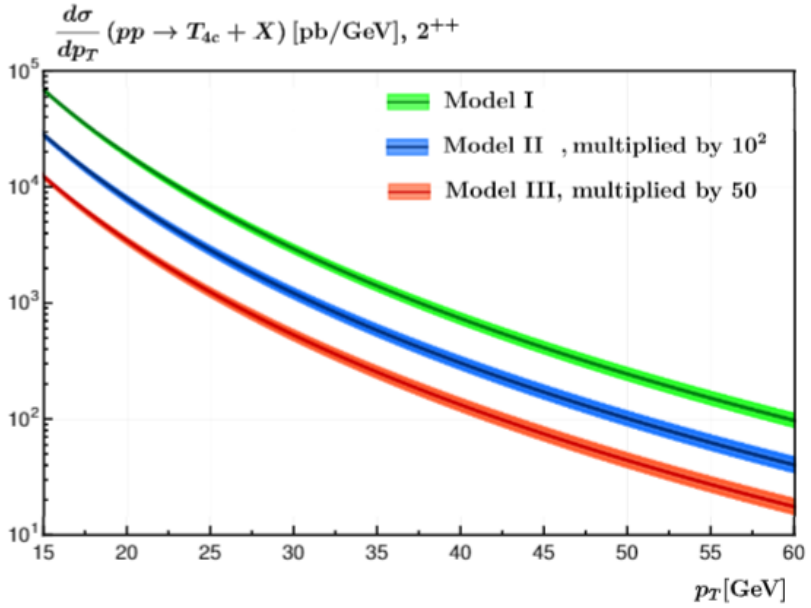

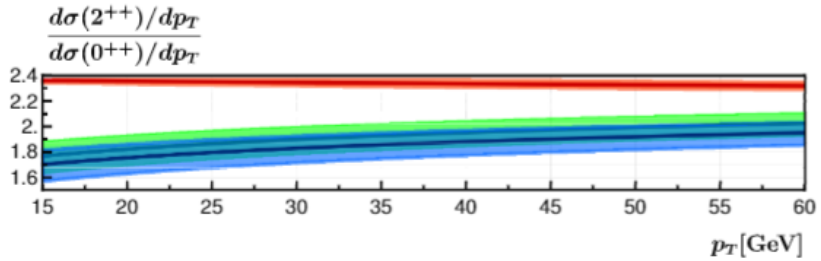

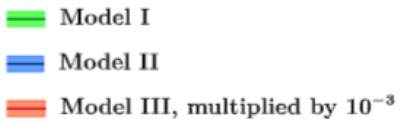

Phenomenology at LHC

- $\sqrt{s} = 13\,\mathrm{TeV}$
- CTEQ14PDF sets
- Factorization scale $\mu \in [m_T/2, 2m_T]$
- $p_T \in [15, 60]\,\mathrm{GeV}$

	0^{++}		2^{++}	
Model	σ/pb	N_{events}	σ/pb	N_{events}
I	1.6×10^5	4.8×10^{11}	2.9×10^5	8.7×10^{11}
II	6.9×10^2	2.1×10^9	1.2×10^3	3.61×10^9
III	0.446	1.3×10^6	1.1×10^3	3.15×10^9

NRQCD Factorization for inclusive production of tetraquark at LHC (fixed-order calculation)

NRQCD Factorization formula for T4c hadroproduction

$$\mathrm{d}\sigma(pp \to T_{4c} + X) = \sum_{i,j=q,g} \int_0^1 dx_1 dx_2 f_{i/p}(x_1, \mu_F)\, f_{j/p}(x_2, \mu_F)\, \mathrm{d}\hat{\sigma}_{ij\to T_{4c}+X}(x_1 x_2 s, \mu_F)$$

$$\frac{\mathrm{d}\hat{\sigma}_{T_{4c}+X}}{\mathrm{d}\hat{t}} = \sum_n \frac{F_n(\hat{s},\hat{t})}{m_c^{14}} (2M_{T_{4c}}) \left\langle O_n^{T_{4c}} \right\rangle,$$

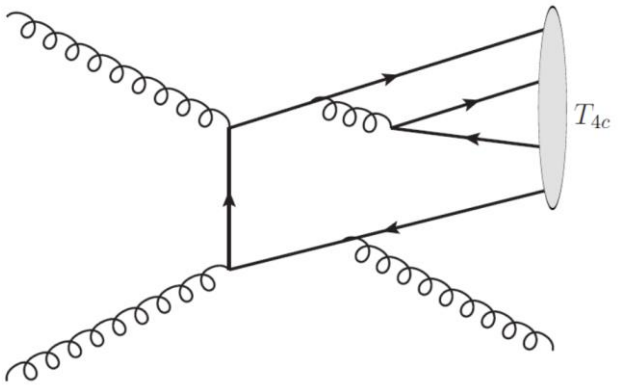

FIG. 1: One typical Feynman diagram for $gg \to T_{4c} + g$.

$$\frac{\mathrm{d}\hat{\sigma}(T_{4c}^{(J)} + X)}{\mathrm{d}\hat{t}} = \frac{2M_{T_{4c}}}{m_c^{14}} \left[F_{3,3}^{(J)} \left\langle O_{3,3}^{(J)} \right\rangle + 2F_{3,6}^{(J)} \left\langle O_{3,6}^{(J)} \right\rangle + F_{6,6}^{(J)} \left\langle O_{6,6}^{(J)} \right\rangle \right]$$

SDCs(asymptotic)

$$F_{3,3}^{0^{++}} = \frac{2209\pi^4 m_c^6 \alpha_s^5 \left(\hat{s}\hat{t}+\hat{s}^2+\hat{t}^2\right)^4}{15552\hat{s}^5(-\hat{t})^3\left(\hat{s}+\hat{t}\right)^3} + \mathcal{O}\left(\frac{m_c^7}{p_T^7}\right),$$

$$F_{3,6}^{0^{++}} = \sqrt{6}F_{3,3}^{0^{++}} + \mathcal{O}\left(\frac{m_c^7}{p_T^7}\right),$$

$$F_{6,6}^{0^{++}} = \frac{2}{3}F_{3,3}^{0^{++}} + \mathcal{O}\left(\frac{m_c^7}{p_T^7}\right),$$

$$F_{3,3}^{1^{+-}} = \frac{60025\pi^4 m_c^8 \alpha_s^5 \left(\hat{s}\hat{t}+\hat{s}^2+\hat{t}^2\right)^2}{34992\hat{s}^4\hat{t}^2\left(\hat{s}+\hat{t}\right)^2} + \mathcal{O}\left(\frac{m_c^9}{p_T^9}\right),$$

$$F_{3,3}^{2^{++}} = \frac{17617\pi^4 m_c^6 \alpha_s^5 \left(\hat{s}\hat{t}+\hat{s}^2+\hat{t}^2\right)^4}{38880\hat{s}^5(-\hat{t})^3\left(\hat{s}+\hat{t}\right)^3} + \mathcal{O}\left(\frac{m_c^7}{p_T^7}\right),$$

All the five SDCs are positive. The partonic cross sections for C-even tetraquarks scale as p_T^{-6} , while those for the C-odd state 1^{+-} scale as p_T^{-8}. At large pT , the predicted LO cross sections for the C-even states receive an extra suppression factor of p_T^{-2} with respect to fragmentation mechanism.

Phenomenology

LDME:

	LDME	Model I [15]	Model II [16]
0^{++}	$\langle O^{(0)}_{3,3} \rangle$ [GeV^9]	0.0347	0.0187
	$\langle O^{(0)}_{3,6} \rangle$ [GeV^9]	0.0211	−0.0161
	$\langle O^{(0)}_{6,6} \rangle$ [GeV^9]	0.0128	0.0139
1^{+-}	$\langle O^{(1)}_{3,3} \rangle$ [GeV^9]	0.0780	0.0480
2^{++}	$\langle O^{(2)}_{3,3} \rangle$ [GeV^9]	0.072	0.0628

	Model I		Model II	
	σ [nb]	$N_{\text{events}}/10^9$	σ [nb]	$N_{\text{events}}/10^9$
0^{++}	37 ± 26	110 ± 80	9 ± 6	27 ± 19
1^{+-}	0.28 ± 0.16	0.8 ± 0.5	0.17 ± 0.10	0.52 ± 0.29
2^{++}	93 ± 65	280 ± 200	81 ± 57	240 ± 170

TABLE II: The integrated production rates for various S-wave T_{4c} states ($6\,\text{GeV} \leq p_T \leq 100\,\text{GeV}$) and the estimated event yields.

Phenomenology

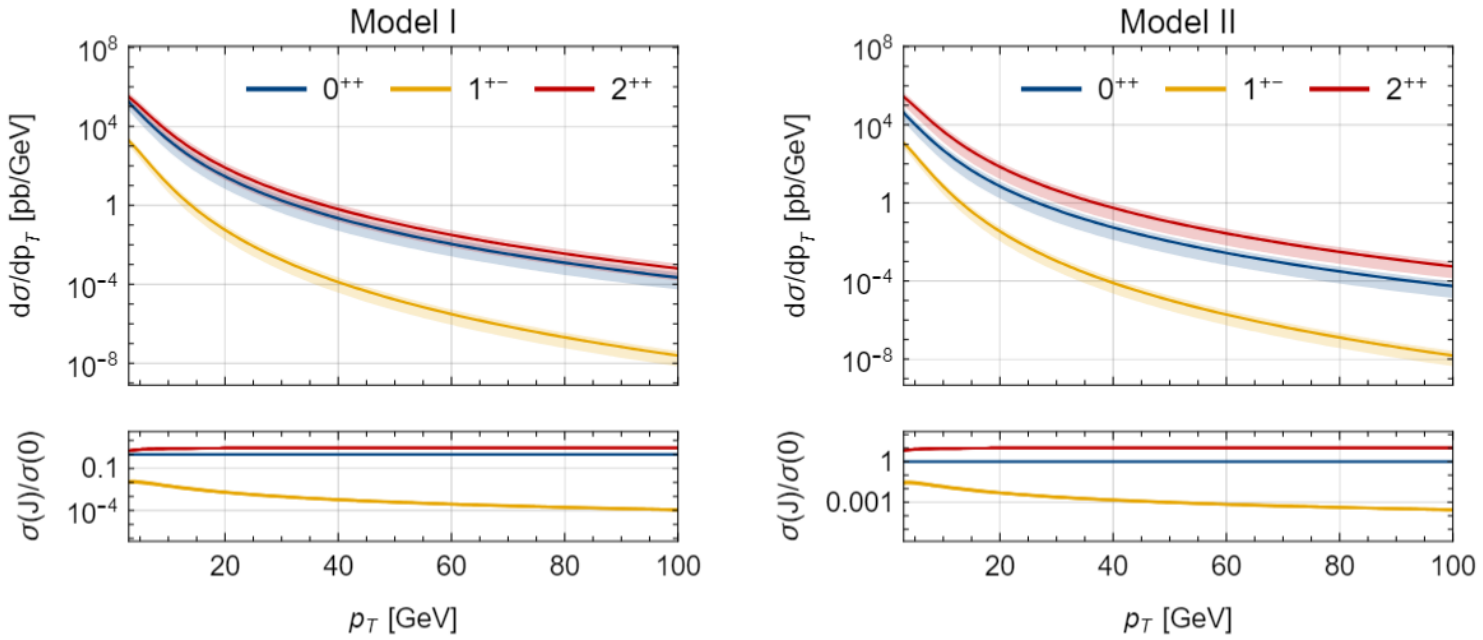

FIG. 2: The p_T spectra of the S-wave T_{4c} at LHC with $\sqrt{s} = 13$ TeV predicted from two potential models. The left panel represents the predictions made from Model I, while the right panel represents the predictions made from Model II. The blue, yellow and red curves represent the differential cross sections for the 0^{++}, 1^{+-} and 2^{++} tetraqaurks, respectively. The lower insets show the ratios of $\sigma(1^{+-})$ and $\sigma(2^{++})$ to $\sigma(0^{++})$.

Phenomenology

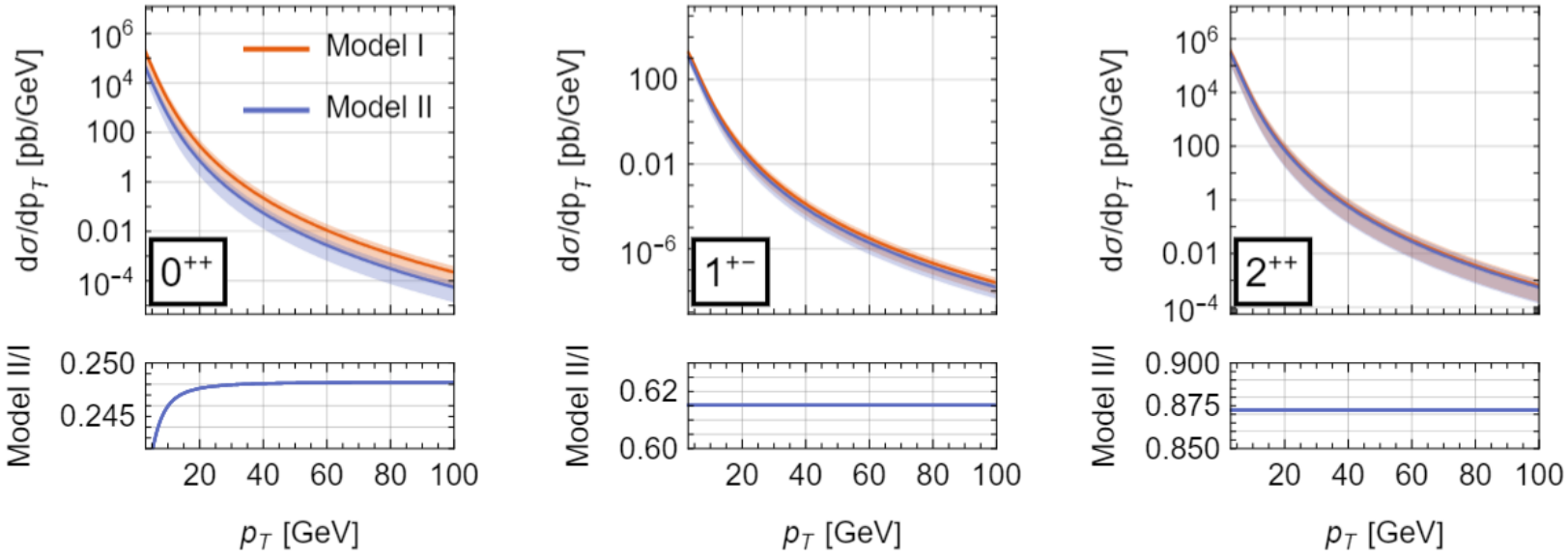

FIG. 3: Comparison of the p_T distributions of the S-wave T_{4c} between two phenomenological potential models. The left, central and right panels represent the differential cross sections for the 0^{++}, 1^{+-} and 2^{++} tetraquarks, respectively. The orange (blue) curves represent the predictions made from Model I (II). The lower insets show the ratios of the predicted production rates in Model II to those in Model I.

Phenomenology

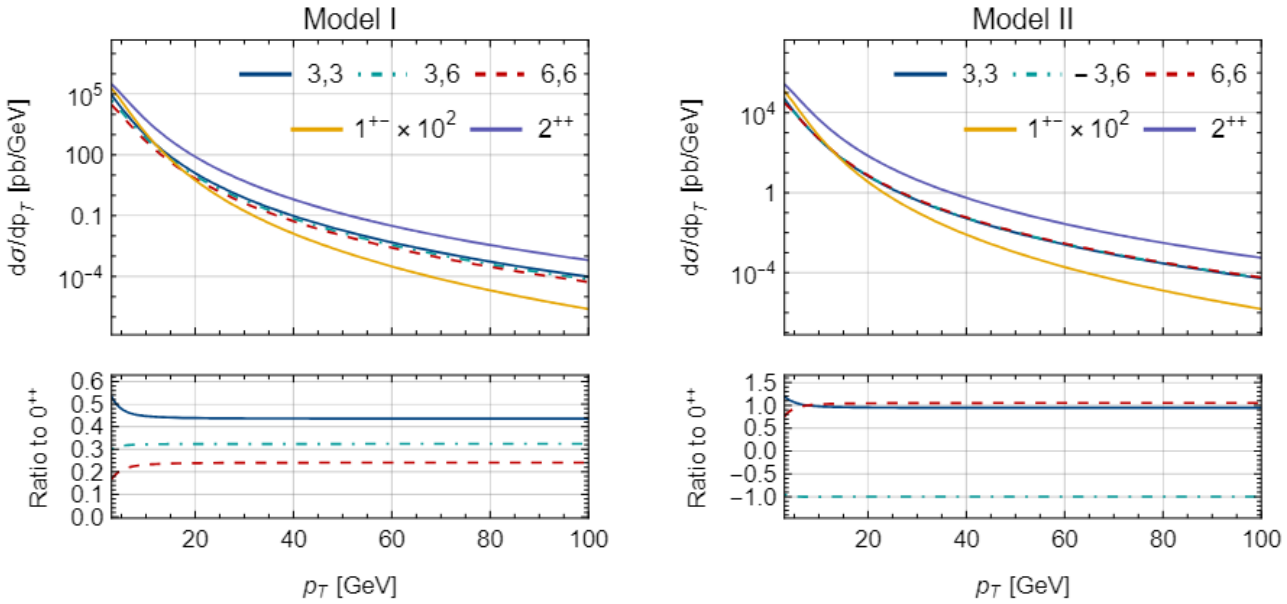

FIG. 4: Comparison of contributions from different color configurations in 3. The left panel is from Model I, and the right panel is for Model II. The blue solid, green dash-dotted and red dashed curves stand for the contributions from the pure color-triplet, interference and pure color-sextet contributions in $\sigma(0^{++})$, respectively. An additional minus sign is added to the interfering term in Model II to make it positive. The lower insets show the ratio of the individual contributions to the full cross section of the 0^{++} tetraquark. We also present the p_T distributions of the 1^{+-} and 2^{++} states for comparison.

Phenomenology

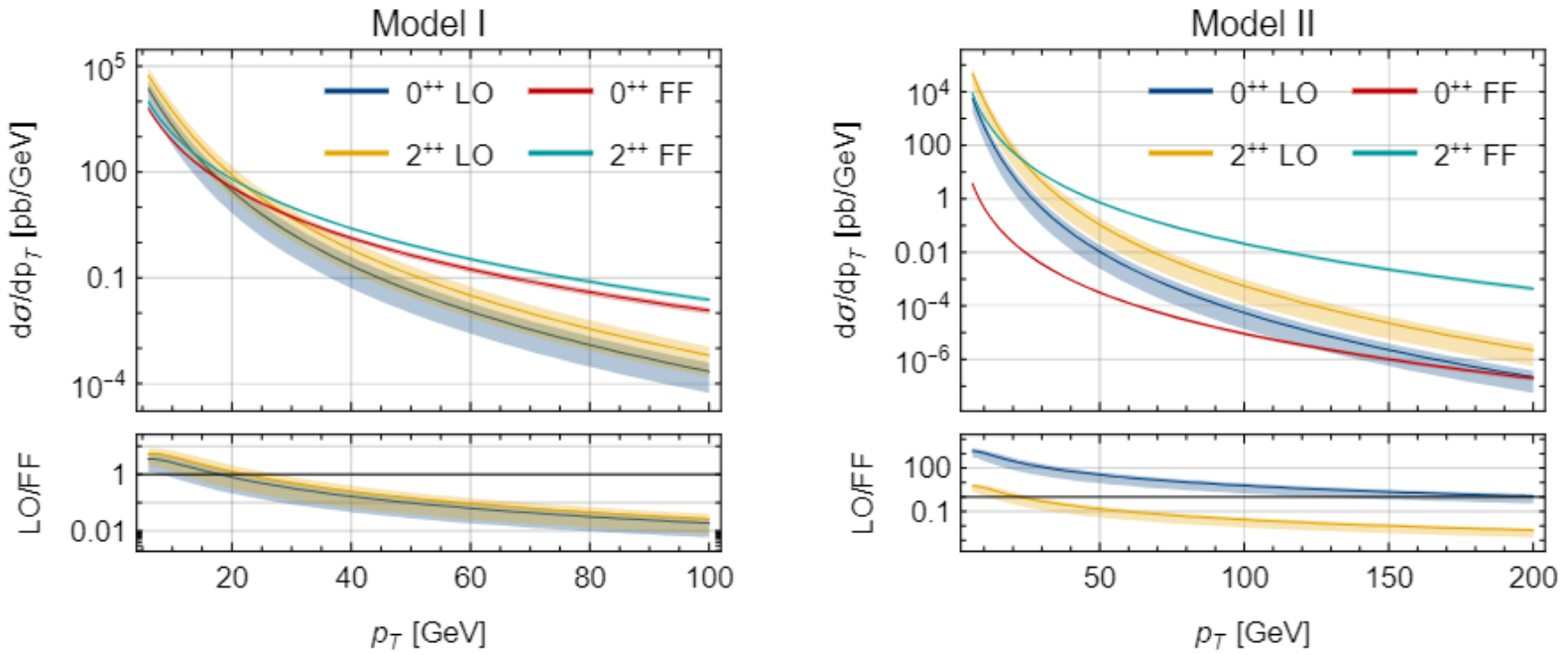

FIG. 5: Comparison of the p_T distributions of the T_{4c} between this work and from the fragmentation mechanism [40]. The left panel is for Model I, and the right panel is from Model II. The blue and yellow curves represent the leading-order NRQCD predictions for $\sigma(0^{++})$ and $\sigma(2^{++})$, while the red and green curves represent the fragmentation contributions to $\sigma(0^{++})$ and $\sigma(2^{++})$. The lower insets show the ratios of the leading-order NRQCD predictions to the fragmentation predictions.

Exclusive production of C-even tetraquark at B factory

There are roughly 40 s-channel diagrams in total.

Due to C-parity conservation, the t-channel process in b) does not contribute.

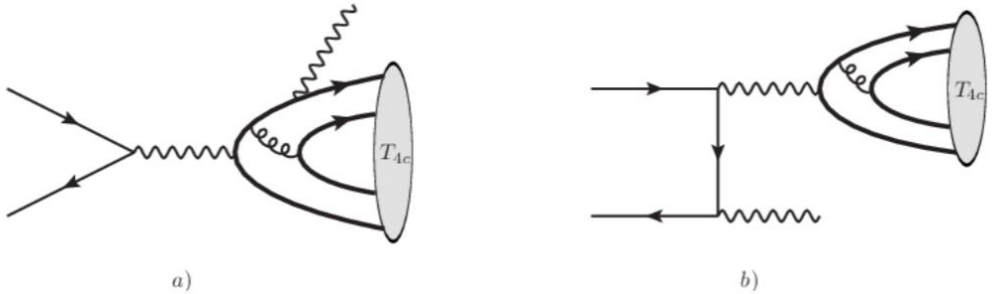

	0^{++}		2^{++}	
Model	σ/fb	$N_{\text{events}}/10^4$	σ/fb	$N_{\text{events}}/10^4$
I	17	86	14	70
II	0.070	0.35	0.058	0.29
III	0.0015	0.0075	0.050	0.25

NRQCD Factorization for inclusive production of 1^{+-} tetraquark at B factory

For the Inclusive production of fully-charmed 1^{+-} tetraquark at B factory

$$d\sigma(e^+e^- \to T_{4c}(E) + X) = \sum_n \frac{\mathrm{d}F_n(E)}{m_c^8}(2M_{T_{4c}})\langle 0|\mathcal{O}_n^{T_{4c}}|0\rangle,$$

$$\mathcal{O}_{\bar{\mathbf{3}}\otimes\mathbf{3}}^{T_{4c}} = \sum_{m_j,X} \mathcal{O}_{\bar{\mathbf{3}}\otimes\mathbf{3}}^{i\dagger}|T_{4c}(m_j) + X\rangle\langle T_{4c}(m_j) + X|\mathcal{O}_{\bar{\mathbf{3}}\otimes\mathbf{3}}^{i},$$

Vacuum-saturation approximation

$$\left\langle 0\left|\mathcal{O}_0^T\right|0\right\rangle \to \sum_X \left\langle 0\left|\mathcal{O}_{\text{color}}^{(J)}\right|T_{4c}^{(J)} + X\right\rangle \left\langle T_{4c}^{(J)} + X\left|\mathcal{O}_{\text{color}}^{(J)\dagger}\right|0\right\rangle \to \left|\left\langle 0\left|\mathcal{O}_{\text{color}}^{(J)}\right|T_{4c}^{(J)}\right\rangle\right|^2$$

Inclusive production of fully-charmed 1^{+-} tetraquark at B factory

There are roughly **400** Feynman diagrams in total.

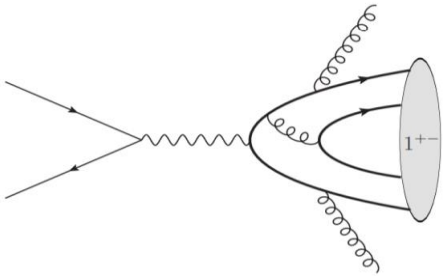

FIG. 1: One of 392 Feynman diagrams for $e^+e^- \to T_{4c}(1^{+-}) + gg$ at $\mathcal{O}(\alpha_s^4)$.

($\sqrt{s} = 10.58\,\mathrm{GeV}$, designed luminosity $\approx 50\,\mathrm{ab}^{-1}$)

Model	$\left\langle T^{(1)}_{\bar{\mathbf{3}}\otimes\mathbf{3}}(m_j) \middle\vert O^{(1)}_{\bar{\mathbf{3}}\otimes\mathbf{3}}(m_j) \middle\vert 0 \right\rangle$	σ/fb	$N_{\mathrm{events}}/10^4$
I	$2.31684\,\mathrm{GeV}^{9/2}$	7.3	37
II	$-0.1612\,\mathrm{GeV}^{9/2}$	0.035	0.18
III	$0.126437\,\mathrm{GeV}^{9/2}$	0.022	0.11

B8. Heavy quarkonium production and decay

Work 1: Photoproduction of C-even quarkonia at EIC and EicC

Y. J, Z. W. Mo, J. C. Pan, and J. Y. Zhang, Photoproduction of C-even quarkonia at EIC and EicC. To appear in PRD [arXiv:2207.14171 [hep-ph]].

Evidence of odderon

Differences between pp and $p\bar{p}$ elastic scattering data at $1.96\ \mathrm{TeV}$ is considered to be the evidence of the Odderon

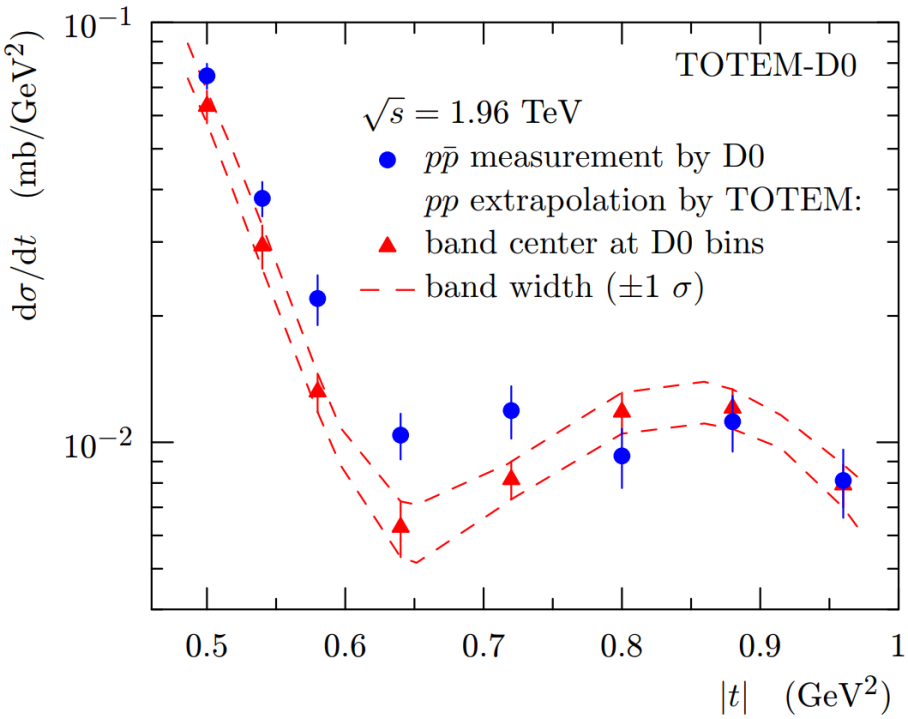

D0 collaboration,
PRL 127 (2021) 6, 062003

Model description of odderon

In perturbative QCD, odderon is denominated by Bartels-Kwiecinski-Praszałowicz(BKP) equation

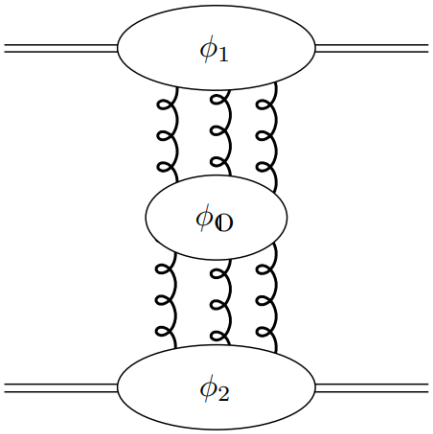

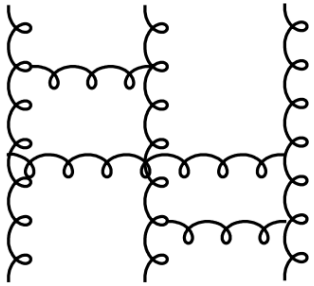

Janik-Wosiek(JW) solution

Bartels– Lipatov–Vacca (BLV) solution

Only BLV solution contributes to photo-production of pseudoscalar meson!

J. Bartels, Nucl. Phys. B 175 (1980) 365
T. Jaroszewicz, Acta Phys. Polon. B 11 (1980) 965
J. Kwiecinski and M. Praszalowicz, Phys. Lett. B 94, 413-416 (1980)

Two mechanisms of photoproduction of C-even quarkonium at EIC/EicC

Odderon exchange:

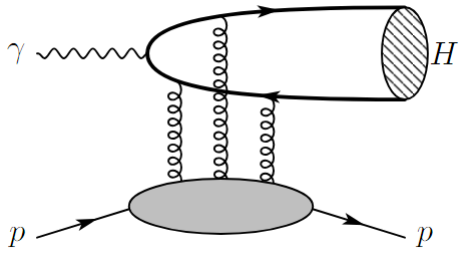

One-photon exchange:

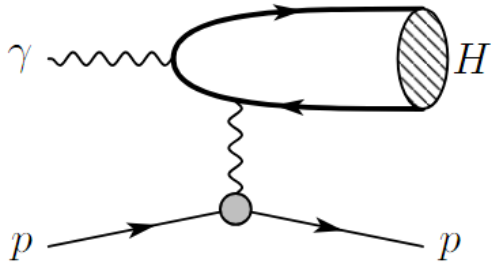

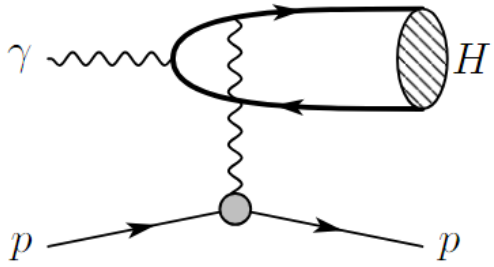

NRQCD factorization of the C-even charmonium photoproduction amplitude

$$\mathcal{M} = \frac{e^2 g_{\mu\nu}}{t} \langle H(P) | J^{\mu}_{\mathrm{EM}} | \gamma(k) \rangle \langle p(P_2) | J^{\nu}_{\mathrm{EM}} | p(P_1) \rangle$$

$$J^{\mu}_{\mathrm{EM}} = \sum_f e_f \bar{q}_f \gamma^{\mu} q_f \qquad H = \eta_c, \chi_{c0,1,2}$$

Nucleon EM form factors measured from experiments

$$\langle p(P_2) | J^{\mu}_{\mathrm{EM}} | p(P_1) \rangle = \bar{u}(P_2) \left[\gamma^{\mu} F_1(q^2) + \frac{i\sigma^{\mu\nu} q_{\nu}}{2M} F_2(q^2) \right] u(P_1)$$

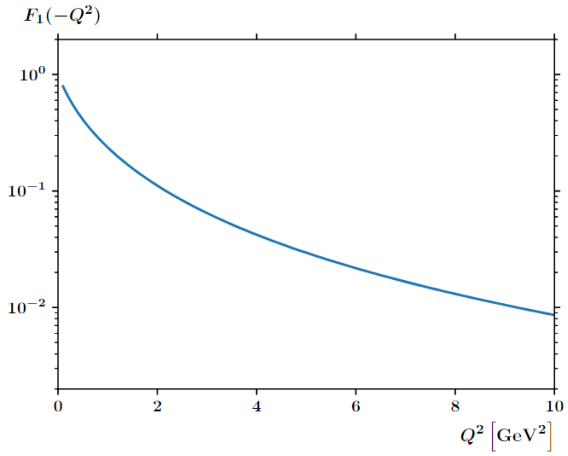

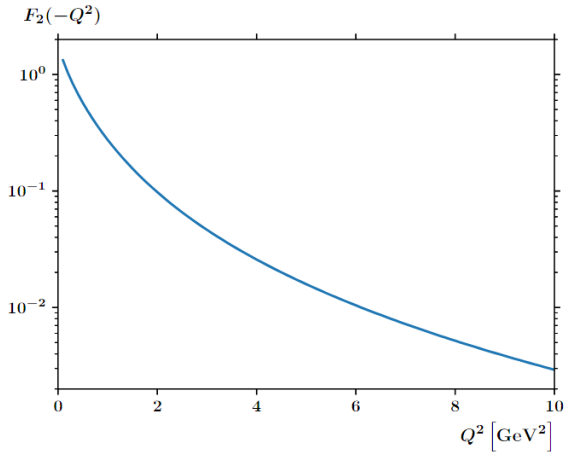

Phys. Lett. B 777, 8-15 (2018)

Photon-to-eta_c EM transition form factor

$$\left\langle \eta_c\left(P\right)\left|J_{\mathrm{EM}}^{\mu}\right|\gamma\left(k\right)\right\rangle = -\frac{4ie_c e}{m_c^{1/2}\left(4m_c^2 - t\right)}\sqrt{\frac{N_c}{2\pi}}R_S\left(0\right)\epsilon^{\mu\nu\rho\sigma}\varepsilon_\nu\left(k\right)k_\rho P_\sigma$$

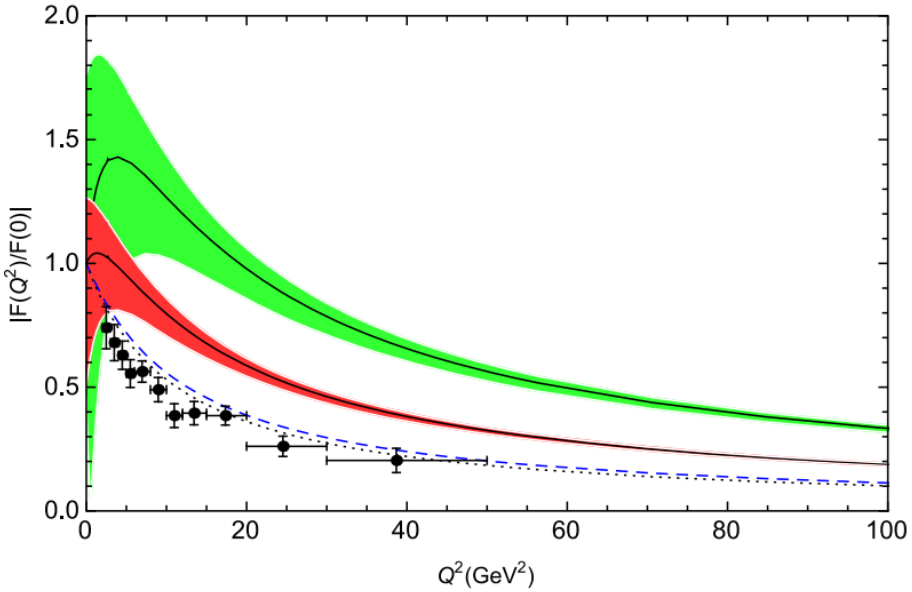

Data from BaBar 2010
Dotted LO
Dashed NLO
Solid NNLO ($\mu_\Lambda = 1$ GeV)
Solid NNLO ($\mu_\Lambda = m$)

Feng, Jia, Sang, PRL 2015

Photon-to-chi_{c0,1,2} EM transition form factor

$$\langle \chi_{c0}(P)|J^{\mu}_{\rm EM}|\gamma(k)\rangle = \frac{2\sqrt{3}e_c e}{3m_c^{3/2}(4m_c^2-t)^2}\sqrt{\frac{3N_c}{2\pi}}R'_P(0)\left(12m_c^2-t\right)$$
$$\times\left[\left(4m_c^2-t\right)g^{\mu\nu}-2k^{\mu}P^{\nu}\right]\varepsilon_{\nu}(k)$$

$$\langle \chi_{c1}(P)|J^{\mu}_{\rm EM}|\gamma(k)\rangle = -\frac{\sqrt{2}ie_c e}{m_c^{5/2}(4m_c^2-t)^2}\sqrt{\frac{3N_c}{2\pi}}R'_P(0)\,\varepsilon^*_{\alpha}(P)\left\{2\left[4m_c^2k^{\mu}+\left(t-4m_c^2\right)P^{\mu}\right]\right.$$
$$\left.\times\,\epsilon^{\nu\rho\sigma\alpha}k_{\rho}P_{\sigma}-2tP^{\nu}\epsilon^{\mu\rho\sigma\alpha}k_{\rho}P_{\sigma}+t\left(4m_c^2-t\right)\epsilon^{\mu\nu\sigma\alpha}P_{\sigma}\right\}\varepsilon_{\nu}(k),$$

$$\langle \chi_{c2}(P)|J^{\mu}_{\rm EM}|\gamma(k)\rangle = \frac{e_c e}{3m_c^{7/2}(4m_c^2-t)^2}\sqrt{\frac{3N_c}{2\pi}}R'_P(0)\,\varepsilon^*_{\alpha\beta}(P)\left\{2m_c^2\left(12m_c^2-t\right)\right.$$
$$\times\left[\left(4m_c^2-t\right)g^{\mu\nu}-2k^{\mu}P^{\nu}\right]g^{\alpha\beta}+96m_c^4g^{\mu\nu}k^{\alpha}k^{\beta}-t\left[\left(4m_c^2-t\right)g^{\mu\nu}-2k^{\mu}P^{\nu}\right]P^{\alpha}P^{\beta}$$
$$-12m_c^2\left[\left(4m_c^2-t\right)g^{\mu\nu}+\left(P^{\mu}-k^{\mu}\right)P^{\nu}\right]\left(k^{\alpha}P^{\beta}+k^{\beta}P^{\alpha}\right)$$
$$+48m_c^4P^{\nu}\left(k^{\alpha}g^{\beta\mu}+k^{\beta}g^{\alpha\mu}\right)-48m_c^4k^{\mu}\left(k^{\alpha}g^{\beta\nu}+k^{\beta}g^{\alpha\nu}\right)$$
$$+6m_c^2\left(4m_c^2-t\right)\left(k^{\mu}+P^{\mu}\right)\left(P^{\alpha}g^{\beta\nu}+P^{\beta}g^{\alpha\nu}\right)$$
$$\left.-24m_c^4\left(4m_c^2-t\right)\left(g^{\alpha\mu}g^{\beta\nu}+g^{\alpha\nu}g^{\beta\mu}\right)\right\}\varepsilon_{\nu}(k),$$

Phenomenological input parameters

$$M_p = 0.938\,\mathrm{GeV}, \quad m_c = 1.5\,\mathrm{GeV}, \quad m_b = 4.7\,\mathrm{GeV}.$$

$$\left|R_{1S(c\bar{c})}\right|^2 = 1.0952\,\mathrm{GeV}^3, \quad \left|R'_{1P(c\bar{c})}(0)\right|^2 = 0.1296\,\mathrm{GeV}^5,$$

$$\left|R_{1S(b\bar{b})}\right|^2 = 5.8588\,\mathrm{GeV}^3, \quad \left|R'_{1P(b\bar{b})}(0)\right|^2 = 1.6057\,\mathrm{GeV}^5.$$

$R^{(\prime)}(0)$: Cornell potential model, from E. J. Eichten and C. Quigg PRD 1995

Regge Limit

$$s \gg 4(m_{c,b})^2, |t_{min}| \ll |t| \ll M_p^2 < 4(m_{c,b})^2$$

$$\frac{d\sigma(\gamma p \to \eta_c p)}{dt} \approx \frac{\pi e_c^4 \alpha^3 N_c |R_S(0)|^2 F_1^2(0)}{m_c^5(-t)},$$

$$\frac{d\sigma(\gamma p \to \chi_{c0} p)}{dt} \approx \frac{9\pi e_c^4 \alpha^3 N_c |R'_P(0)|^2 F_1^2(0)}{m_c^7(-t)},$$

$$\frac{d\sigma(\gamma p \to \chi_{c1} p)}{dt} \approx \frac{3\pi e_c^4 \alpha^3 N_c |R'_P(0)|^2 F_1^2(0)}{m_c^9},$$

$$\frac{d\sigma(\gamma p \to \chi_{c2} p)}{dt} \approx \frac{12\pi e_c^4 \alpha^3 N_c |R'_P(0)|^2 F_1^2(0)}{m_c^7(-t)}.$$

Landau-Yang theorem indicates that chi_c1 production rate is Heavily suppressed

Threshold Limit

$$\frac{d\sigma\left(\gamma p\to\eta_c p\right)}{dt}\approx\frac{\pi e_c^4\alpha^3 N_c\left|R_S\left(0\right)\right|^2\left(F_1(t_0)+F_2(t_0)\right)^2(M_p+2m_c)}{8M_p m_c^5(M_p+m_c)^2},$$

$$\frac{d\sigma\left(\gamma p\to\chi_{c0} p\right)}{dt}\approx\frac{\pi e_c^4\alpha^3 N_c\left|R'_P\left(0\right)\right|^2\left(F_1(t_0)+F_2(t_0)\right)^2(M_p+2m_c)(2M_p+3m_c)^2}{8M_p m_c^7(M_p+m_c)^4}$$

$$\begin{aligned}\frac{d\sigma\left(\gamma p\to\chi_{c1} p\right)}{dt}\approx&\frac{3\pi e_c^4\alpha^3 N_c\left|R'_P\left(0\right)\right|^2\left(M_p+2m_c\right)}{16M_p m_c^9(M_p+m_c)^4}\left(F_1^2(t_0)M_p^2\left(M_p^2+4M_p m_c+5m_c^2\right)\right.\\&\left.-4F_1(t_0)F_2(t_0)M_p m_c^3+F_2^2(t_0)m_c^2\left(M_p^2+m_c^2\right)\right),\end{aligned}$$

$$\begin{aligned}\frac{d\sigma\left(\gamma p\to\chi_{c2} p\right)}{dt}\approx&\frac{\pi e_c^4\alpha^3 N_c\left|R'_P\left(0\right)\right|^2\left(M_p+2m_c\right)}{16M_p m_c^9(M_p+m_c)^4}\\&\times\left(F_1^2(t_0)\left(3M_p^4+12M_p^3m_c+19M_p^2m_c^2+24M_p m_c^3+24m_c^4\right)\right.\\&+4F_1(t_0)F_2(t_0)m_c^2\left(2M_p^2+9M_p m_c+12m_c^2\right)\\&\left.+F_2^2(t_0)m_c^2\left(7M_p^2+24M_p m_c+27m_c^2\right)\right).\end{aligned}$$

$$t_0=-4M_p m_c^2/(M_p+2m_c)$$

In threshold limit, the differential cross section is isotropic and integrated cross section is suppressed by relative velocity of proton and quarkonium $\sqrt{s-(M_P+M_H)^2}$

Differential & integrated Cross Sections

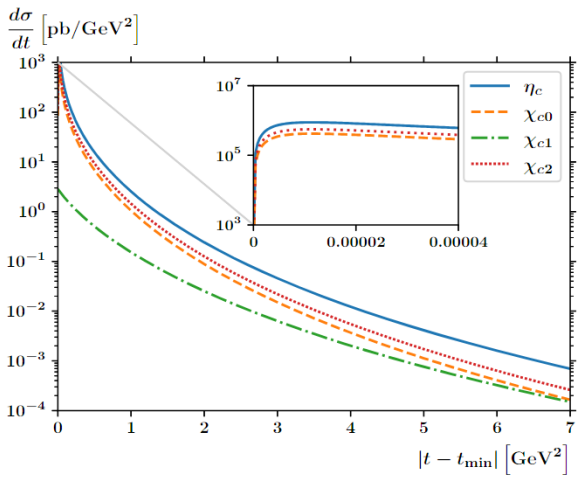

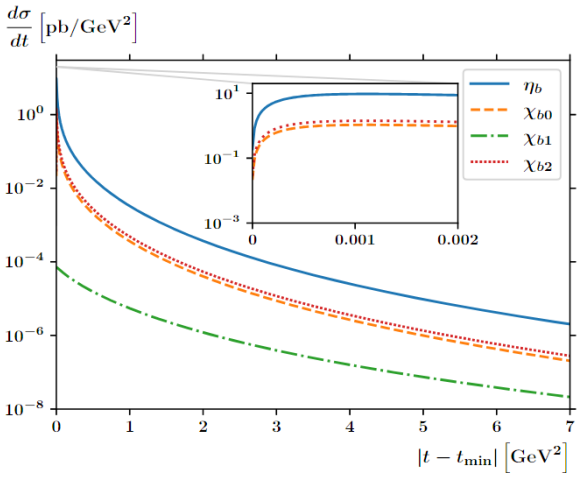

$\sqrt{s} = 50$ GeV

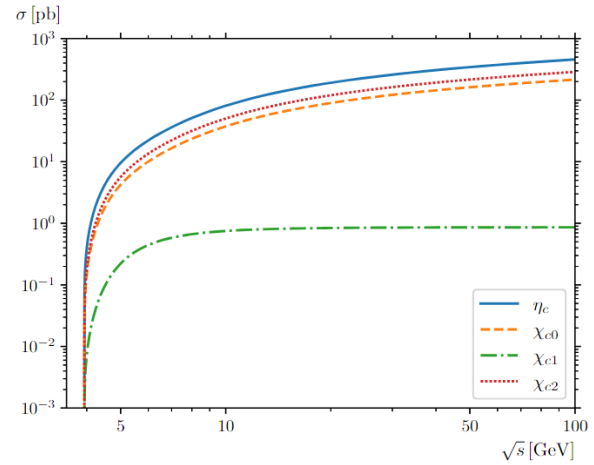

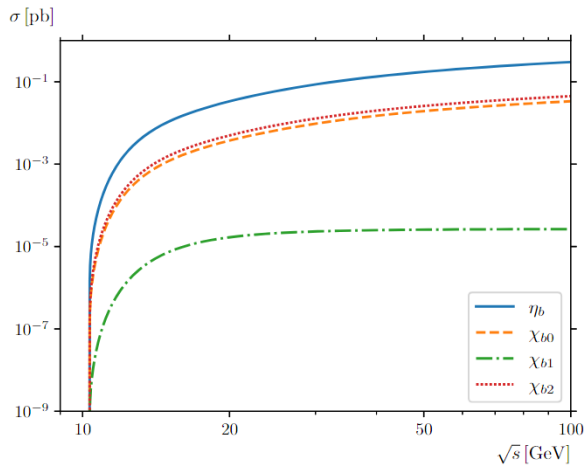

(a) charmonia

(b) bottomonia

Comparison between the one-photon exchange and the odderon exchange model

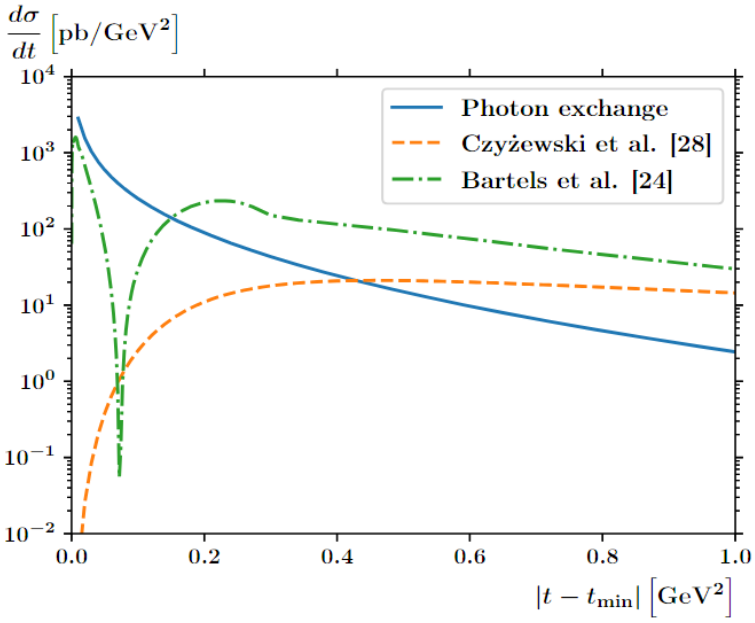

(a) $\sqrt{s} = 15$ GeV

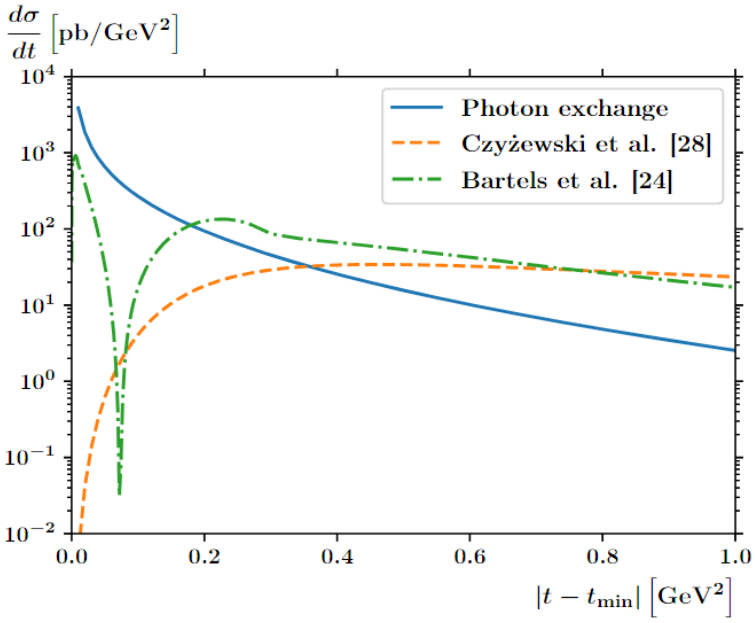

(b) $\sqrt{s} = 50$ GeV

Lesson: even in the Regge limit, one-photon exchange appears to be as important as the odderon contribution, thus non-negligible

Observation prospects in the forthcoming EIC/EicC

Equivalent Photon appr.

$$\sigma\left(ep \to eHp\right) \approx \int_{k_{\min}}^{E_e} dk \int_{Q_{\min}}^{Q_{\max}} dQ^2 \frac{d^2N_\gamma}{dkdQ^2} \sigma\left(\gamma p \to Hp\right)$$

$$\frac{d^2N_\gamma}{dkdQ^2} = \frac{\alpha}{\pi k Q^2}\left[1 - \frac{k}{E_e} + \frac{k^2}{2E_e^2} - \left(1 - \frac{k}{E_e}\right)\frac{Q_{\min}^2}{Q^2}\right]$$

where k and E_e are the photon and electron energies in the target rest frame. $k_{\min} = E_e M_H \left(M_H + 2M_p\right) / \left(s - M_p^2\right)$, $Q_{\min}^2 = m_e^2 k^2 / \left(E_e \left(E_e - k\right)\right)$. We choose $Q_{\max}^2 = 0.01\ \mathrm{GeV}^2$

Take $\chi_{c(b)0}$ as an example. Considering typical center-of-mass energy at EIC, we find that the photoproduction rates in ep collision can reach 7.5 pb for χ_{c0} and 0.35 fb for χ_{b0}

Expected to have enough number of events!

Integrated luminosity of EIC: 1.5 fb^{-1}/month

Integrated luminosity of EicC: 50 fb^{-1}/year

C-even quarkonia photoproduction processes have a bright prospect to be observed in the future EicC and EIC experiments!!

B8. Heavy quarkonium production and decay

Work 2: Two-loop QCD corrections exclusive double charmonium production at B factorie

Sang, Feng, **Y. J**, Mo, Pan and Zhang, Optimized $\mathcal{O}({\alpha_s}^2)$ correction to exclusive double J/φ production at B factories. [arXiv:2306.11538 [hep-ph]].

Sang, Feng, **Y.J.**, Mo and Zhang, $\mathcal{O}({\alpha_s}^2)$ corrections to $J/\varphi + \chi_{c0,1,2}$ production at B factories, Phys. Lett. B 843, 138057. (2023)

Sang, Feng, **Y.J.**, Mo and Zhang, Next-to-next-to-leading-order QCD corrections to $e^+e^- \to J/\varphi + \eta_c$ at B factories. [arXiv:1901.08447 [hep-ph]] (updated in 2022)

Observation of double charmonium production at B factories at the beginning of this century stimulates lots of interest

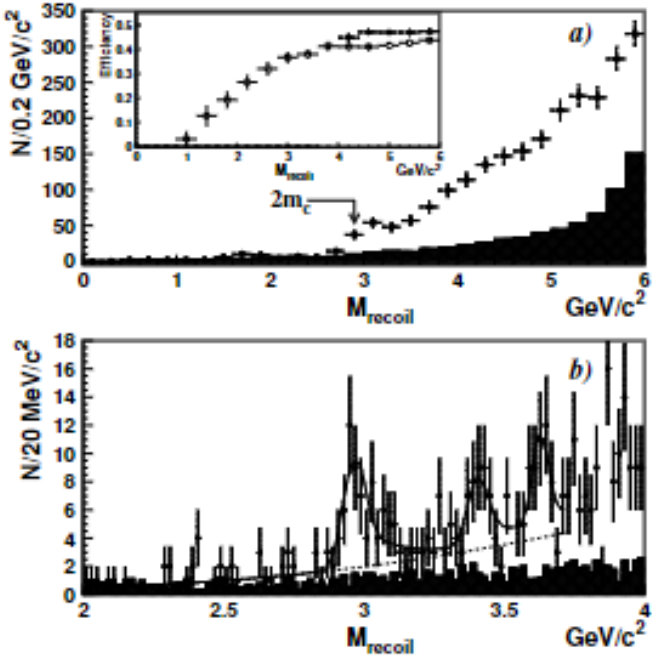

- $\sigma\,(J/\psi + \eta_c)$
  - $\sigma \times \mathcal{B}_{>4} = 33^{+7}_{-6} \pm 9\,\text{fb}$ @Belle[1]
  - $\sigma \times \mathcal{B}_{>2} = 25.6 \pm 2.8 \pm 3.4\,\text{fb}$ @Belle[2]
  - $\sigma \times \mathcal{B}_{>2} = 17.6 \pm 2.8^{+1.5}_{-2.1}\,\text{fb}$ @BaBar[3]
- $\sigma\,(J/\psi + \chi_{c0})$
  - $\sigma \times \mathcal{B}_{>2} = 6.4 \pm 1.7 \pm 1.0\,\text{fb}$ @Belle[2]
  - $\sigma \times \mathcal{B}_{>2} = 10.3 \pm 2.5^{+1.4}_{-1.8}\,\text{fb}$ @BaBar[3]
- $\sigma\,(J/\psi + \chi_{c1}) + \sigma\,(J/\psi + \chi_{c2})$
  - $\sigma \times \mathcal{B}_{>2} < 5.3\,\text{fb}$ at 90%C.L. @Belle[2]

Belle, BaBar, 2002

Next-to-next-to-leading-order QCD corrections to $e^+e^- \to J/\psi + \eta_c$ at B factories

The cross section can be further divided into the $\mathcal{O}(v^0)$ and $\mathcal{O}(v^2)$ pieces

$$\sigma[e^+e^- \to J/\psi + \eta_c] = \frac{4\pi\alpha^2}{3}\left(\frac{|\mathbf{P}|}{\sqrt{s}}\right)^3 |F(s)|^2$$
$$= \sigma_0 + \sigma_2 + \mathcal{O}(\sigma_0 v^4),$$

$$\sigma_0 = \frac{8\pi\alpha^2 m^2 (1-4r)^{3/2}}{3}\langle\mathcal{O}\rangle_{J/\psi}\langle\mathcal{O}\rangle_{\eta_c}|f|^2$$

$$\sigma_2 = \frac{4\pi\alpha^2 m^2 (1-4r)^{3/2}}{3}\langle\mathcal{O}\rangle_{J/\psi}\langle\mathcal{O}\rangle_{\eta_c}$$
$$\times \sum_{H=J/\psi,\eta_c}\left(\frac{1-10r}{1-4r}|f|^2 + 4\,\mathrm{Re}(f g_H^*)\right)\langle v^2\rangle_H,$$

$$r = 4m^2/s$$

Short-distance coefficients

$$|f|^2 = \left|f^{(0)}\right|^2 + \frac{\alpha_s}{\pi} 2\mathrm{Re}\left(f^{(0)} f^{(1)*}\right) + \left(\frac{\alpha_s}{\pi}\right)^2 \left[2\mathrm{Re}\left(f^{(0)} f^{(2)*}\right) + \left|f^{(1)}\right|^2\right],$$

Tree level

$$f^{(0)} = \frac{32\pi C_F e_c \alpha_s}{N_c m s^2},$$

$$g^{(0)}_{J/\psi} = \frac{3-10r}{6} f^{(0)}, \quad g^{(0)}_{\eta_c} = \frac{2-5r}{3} f^{(0)},$$

$\mathcal{O}(\alpha_s^2)$

$$f^{(2)} = f^{(0)} \left\{ \frac{\beta_0^2}{16} \ln^2 \frac{s}{4\mu_R^2} - \left(\frac{\beta_1}{16} + \frac{1}{2}\beta_0 \hat{f}^{(1)}\right) \ln \frac{s}{4\mu_R^2} + (\gamma_{J/\psi} + \gamma_{\eta_c}) \ln \frac{\mu_\Lambda^2}{m^2} + \mathrm{F}(r) \right\}.$$

Calculating the SDCs

Nearly 2000 two-loop diagrams。

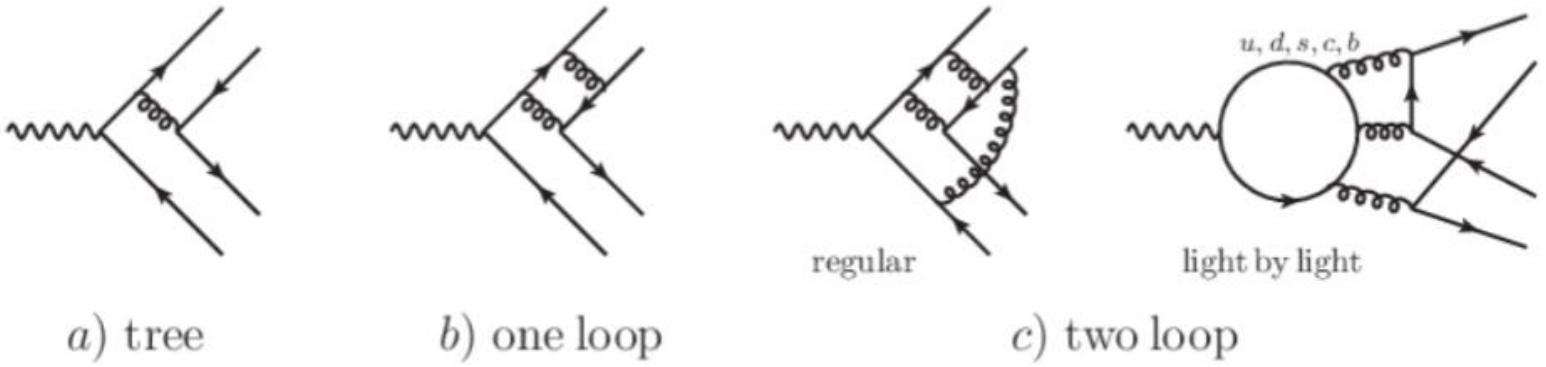

"Light-by-light" amplitudes stemming from the light quark loops cancels.

A powerful new package AMFlow allows to compute complicated master integrals accurately

Y. Q. Ma and X. Liu 2019, 2021

700 MIs by Auxiliary-Mass-Flow method (AMFlow)

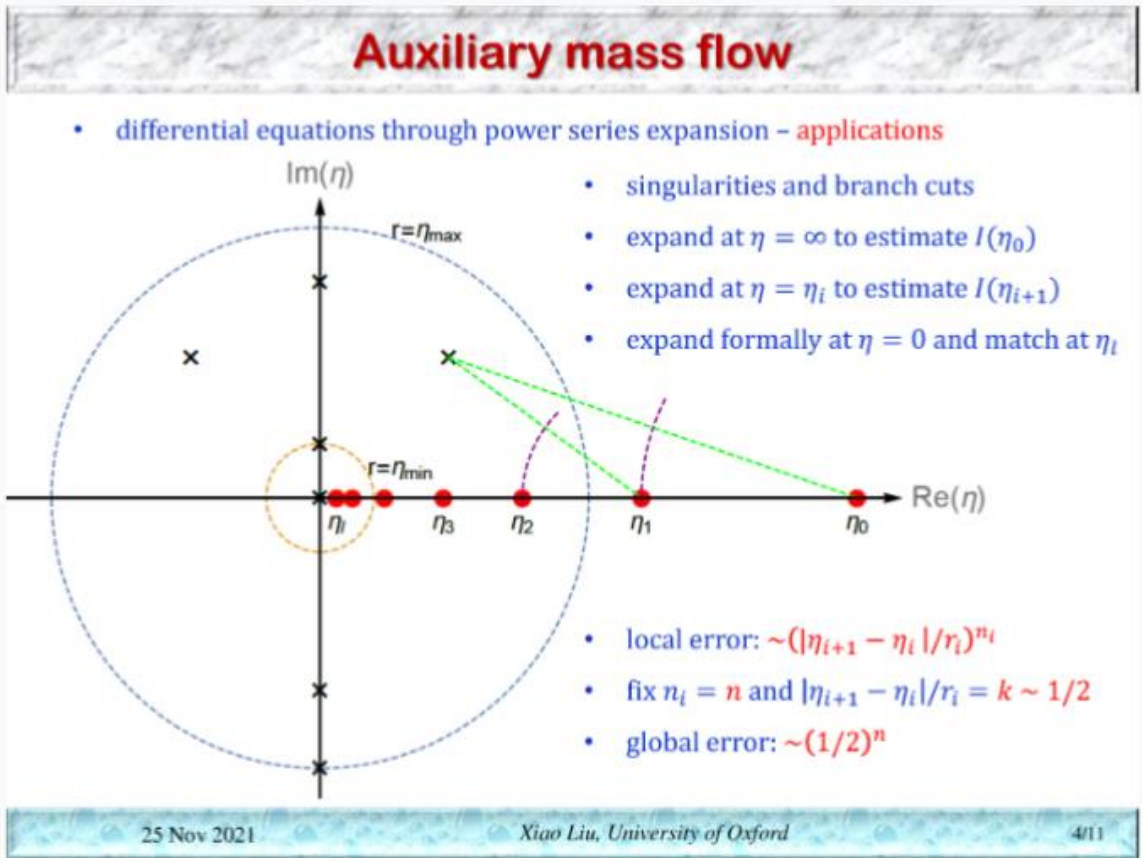

Cross sections up to NNLO

$\sigma[e^+e^- \to J/\psi+\eta_c]$ (in units of fb) at $\sqrt{s} = 10.58$ GeV. $\mu_\Lambda = 1$ GeV

m(GeV)	μ_R	LO	NLO	NNLO
1.5	$\sqrt{s}/2$	$5.05^{+0.92+2.31}_{-0.99-1.49}$	$10.54^{+2.86+3.92}_{-2.60-2.66}$	$15.00^{+5.03+4.29}_{-4.14-3.14}$

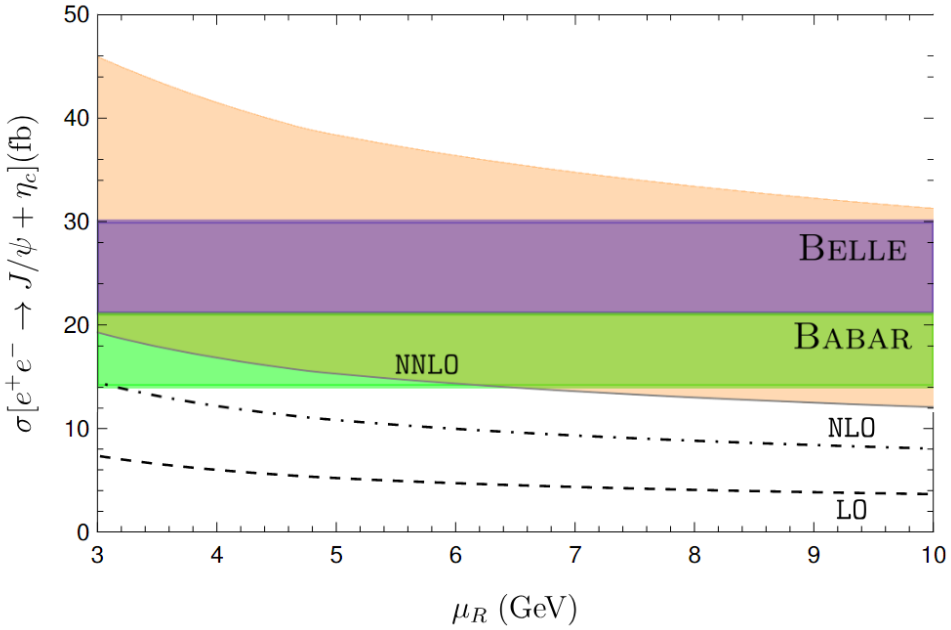

Belle:

$\sigma[J/\psi + \eta_c] \times \mathcal{B}_{>2} = 25.6 \pm 2.8 \pm 3.4$ fb

Babar:

$\sigma[J/\psi + \eta_c] \times \mathcal{B}_{>2} = 17.6 \pm 2.8^{+1.5}_{-2.1}$ fb

$\mathcal{O}(\alpha_s^2)$ corrections to $e^+e^- \to J/\psi + \chi_{cJ}$ at B Factories

The process is decomposed to decay of the photon and expressed as helicity amplitudes

$$\frac{\mathrm{d}\sigma\left[e^+e^- \to J/\psi(\lambda_1) + \chi_{cJ}(\lambda_2)\right]}{\mathrm{d}\cos\theta} = \frac{\alpha|\mathbf{P}||\mathcal{A}^J_{\lambda_1,\lambda_2}|^2}{8s^{5/2}} \times \begin{cases} \dfrac{1+\cos^2\theta}{2}, & \lambda = \pm 1, \\ 1-\cos^2\theta, & \lambda = 0, \end{cases}$$

Factorization holds at helicity amplitude level

NRQCD Factorization Formula

$$\mathcal{A}^J_{\lambda_1,\lambda_2} = \mathcal{C}^J_{\lambda_1,\lambda_2} \frac{\langle J/\psi|\psi^\dagger \boldsymbol{\sigma}\cdot\boldsymbol{\varepsilon}_{J/\psi}\chi(\mu_\Lambda)|0\rangle\langle\chi_{cJ}|\psi^\dagger\mathcal{K}_{^3P_J}\chi(\mu_\Lambda)|0\rangle}{m_c^3} + \mathcal{O}\left(v^2\right).$$

$$\mathcal{K}_{^3P_0} = \frac{1}{\sqrt{3}}\left(-\frac{\mathrm{i}}{2}\overleftrightarrow{\mathbf{D}}\cdot\boldsymbol{\sigma}\right), \quad \mathcal{K}_{^3P_1} = \frac{1}{\sqrt{2}}\left(-\frac{\mathrm{i}}{2}\overleftrightarrow{\mathbf{D}}\times\boldsymbol{\sigma}\right)\cdot\boldsymbol{\varepsilon}_{\chi c1}, \quad \mathcal{K}_{^3P_2} = -\frac{\mathrm{i}}{2}\overleftrightarrow{D}^{(i}\sigma^{j)}\varepsilon^{ij}_{\chi c2}$$

Short-Distantce Coefficients(SDCs)

Through $\mathcal{O}(\alpha_s^2)$, **dimensionless** SDC is expected to take the following structure:

$$\mathcal{C}^{J}_{\lambda_1,\lambda_2}\left(r,\frac{\mu_R^2}{m_c^2},\frac{\mu_\Lambda^2}{m_c^2}\right)=\frac{64\pi e\alpha_s}{27\sqrt{3}}r^{(1+|\lambda_1+\lambda_2|)/2}\mathcal{C}^{J(\text{tree})}_{\lambda_1,\lambda_2}\left\{1+\frac{\alpha_s(\mu_R)}{\pi}\left(\frac{1}{4}\beta_0\ln\frac{\mu_R^2}{m_c^2}+c^{J(1)}_{\lambda_1,\lambda_2}\right)\right.$$
$$+\frac{\alpha_s^2(\mu_R)}{\pi^2}\left(\frac{1}{16}\beta_0^2\ln^2\frac{\mu_R^2}{m_c^2}+\frac{1}{16}(8c^{J(1)}_{\lambda_1,\lambda_2}\beta_0+\beta_1)\ln\frac{\mu_R^2}{m_c^2}\right.$$
$$\left.\left.+(\gamma_{J/\psi}+\gamma_{\chi_{cJ}})\ln\frac{\mu_\Lambda^2}{m_c^2}+\boxed{c^{J(2)}_{\lambda_1,\lambda_2}}\right)\right\},\quad r:=\frac{4m_c^2}{s}$$

- (LO) $\mathcal{C}^{J(\text{tree})}_{\lambda_1,\lambda_2}$: *Braaten, Lee, PRD2003*
- (NLO) $c^{J(1)}_{\lambda_1,\lambda_2}$: *Zhang, Ma, Chao, PRD2008; Wang, Ma, Chao, PRD2011; Dong, Feng, Jia, JHEP2011.*

IR Divergence factored into NRQCD matrix element

Renormalized quark helicity amplitude is left with a single IR pole, as inferred by NRQCD factorization

$$\gamma_{J/\psi} = -\pi^2\left(\frac{C_A C_F}{4} + \frac{C_F^2}{6}\right),$$
$$\gamma_{\chi_{c0}} = -\pi^2\left(\frac{C_A C_F}{12} + \frac{C_F^2}{3}\right),$$
$$\gamma_{\chi_{c1}} = -\pi^2\left(\frac{C_A C_F}{12} + \frac{5C_F^2}{24}\right),$$
$$\gamma_{\chi_{c2}} = -\pi^2\left(\frac{C_A C_F}{12} + \frac{13C_F^2}{120}\right).$$

These IR divergences indicate highly nontrivial test of NRQCD factorization for exclusive S + P -wave charmonium production at two loop order.

Various NRQCD short-distance coefficients

√s = 10.58 GeV,
mc = 1.5 GeV,
mb = 4.7 GeV

H	(λ_1, λ_2)	$c^{(2)}_{\lambda_1,\lambda_2}$
χ_{c0}	$(1,0)$	$-34.73+9.11i+(-0.8042+0.2182i)n_L+(-0.2687-0.0821i)n_L^2$ $+(-0.2046+0.1862i)\mathrm{lbl}_c+(-0.0249+0.1891i)\mathrm{lbl}_b$
	$(0,0)$	$-46.10+19.02i+(0.3140-0.2819i)n_L+(-0.2765-0.0432i)n_L^2$ $+(-0.2688+0.2705i)\mathrm{lbl}_c+(-0.0394+0.1948i)\mathrm{lbl}_b$
χ_{c1}	$(1,1)$	$-81.86-46.54i+(3.924+5.361i)n_L+(-0.2781-0.0349i)n_L^2$ $+(0.2566-0.0907i)\mathrm{lbl}_c+(0.4657+0.0763i)\mathrm{lbl}_b$
	$(1,0)$	$-626.7-416.2i+(56.22+25.82i)n_L+(-0.2632-0.1095i)n_L^2$ $+(0.2721+0.9668i)\mathrm{lbl}_c+(2.755+1.772i)\mathrm{lbl}_b$
	$(0,1)$	$-48.57-18.06i+(0.814+2.847i)n_L+(-0.2793-0.0290i)n_L^2$ $+(0.1354-0.0549i)\mathrm{lbl}_c+(0.2120-0.0063i)\mathrm{lbl}_b$
χ_{c2}	$(1,2)$	$-49.95-11.46i+(4.387+2.203i)n_L+(-0.2632-0.1095i)n_L^2$ $+(-0.7295+0.3095i)\mathrm{lbl}_c+(-0.5207+0.3913i)\mathrm{lbl}_b$
	$(1,1)$	$-72.48-1.12i+(3.243+2.181i)n_L+(-0.2781-0.0349i)n_L^2$ $+(-0.2593+0.1258i)\mathrm{lbl}_c+(-0.1398+0.1887i)\mathrm{lbl}_b$
	$(1,0)$	$-59.64-9.29i+(2.137+2.167i)n_L+(-0.2852+0.0006i)n_L^2$ $+(-0.2415+0.1598i)\mathrm{lbl}_c+(-0.1002+0.1359i)\mathrm{lbl}_b$
	$(0,1)$	$-19.35-22.71i+(1.512+1.247i)n_L+(-0.3052+0.1005i)n_L^2$ $+(0.1925+0.0292i)\mathrm{lbl}_c+(0.2658-0.1131i)\mathrm{lbl}_b$
	$(0,0)$	$-66.01-27.27i+(4.373+1.358i)n_L+(-0.3002+0.0755i)n_L^2$ $+(-0.1245+0.2091i)\mathrm{lbl}_c+(0.02997-0.00909i)\mathrm{lbl}_b$

μ_Λ NRQCD factorization scale dependence

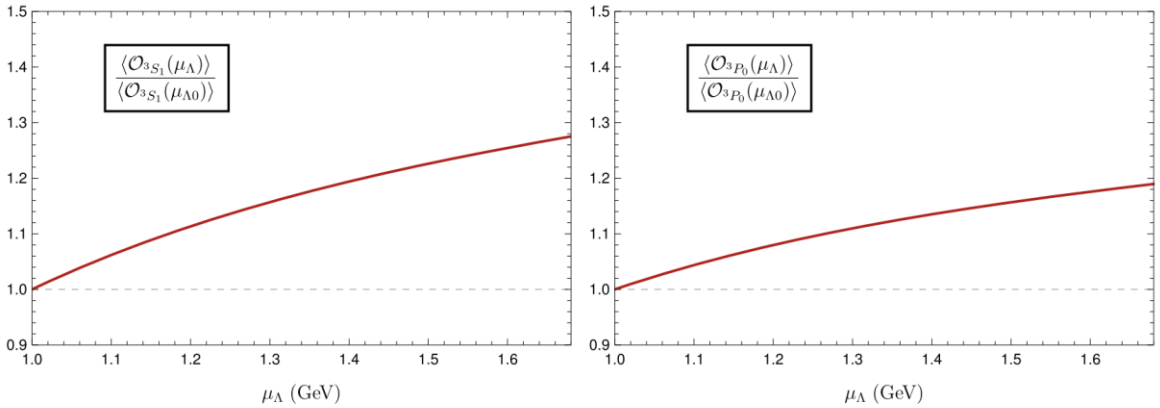

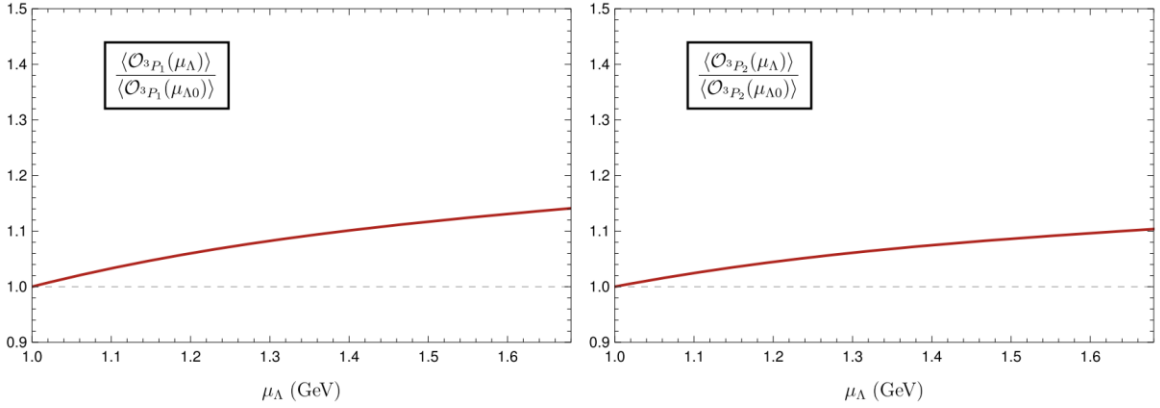

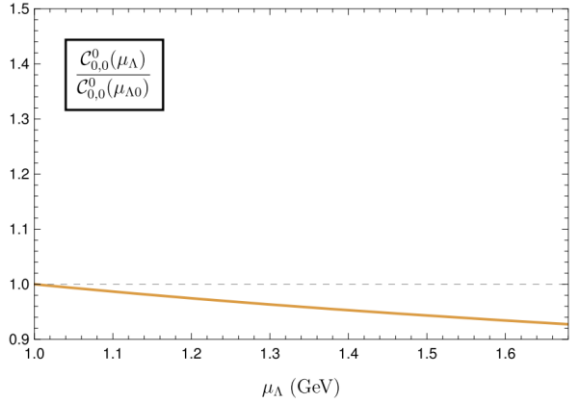

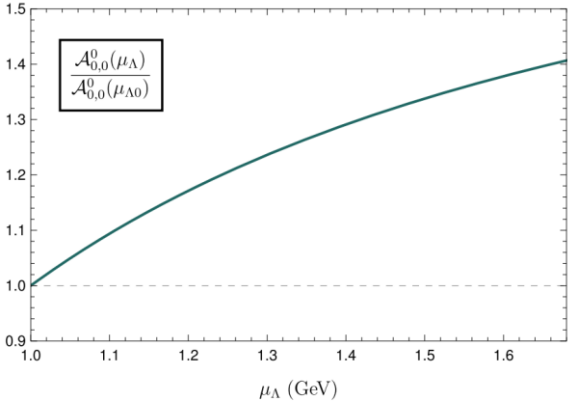

Unpolarized Cross Sections

Comparison between our finest predictions to the unpolarized cross sections and the measurements in two B factories (in units of fb)

$$\left|R_{J/\psi}(0)\right|^2 = 0.81\ \text{GeV}^3, \quad \left|R_{\psi(2S)}(0)\right|^2 = 0.529\ \text{GeV}^3, \quad \left|R'_{\chi_{cJ}}(0)\right|^2 = 0.075\ \text{GeV}^5.$$

	LO	NLO	NNLO	Belle $\sigma \times \mathcal{B}_{>2(0)}$ [56]	BaBar $\sigma \times \mathcal{B}_{>2}$ [2]
$\sigma(J/\psi + \chi_{c0})$	$3.35^{+1.14}_{-0.99}$	$6.05^{+1.13}_{-1.17}$	$10.45^{+0.11\,+2.60}_{-0.58\,-3.87}$	$6.4 \pm 1.7 \pm 1.0$	$10.3 \pm 2.5^{+1.4}_{-1.8}$
$\sigma(J/\psi + \chi_{c1})$	$0.503^{+0.172}_{-0.148}$	$0.63^{+0.08}_{-0.09}$	$0.867^{+0.006\,+0.188}_{-0.005\,-0.291}$	–	–
$\sigma(J/\psi + \chi_{c2})$	$0.64^{+0.22}_{-0.19}$	$0.72^{+0.04}_{-0.07}$	$0.728^{+0.123\,+0.121}_{-0.161\,-0.212}$	–	–
$\sigma(J/\psi + \chi_{c1}) + \sigma(J/\psi + \chi_{c2})$	$1.15^{+0.39}_{-0.34}$	$1.36^{+0.12}_{-0.16}$	$1.60^{+0.12\,+0.31}_{-0.17\,-0.50}$	<5.3 at 90% C.L.	–
$\sigma(\psi(2S) + \chi_{c0})$	$2.19^{+0.75}_{-0.64}$	$3.95^{+0.74}_{-0.76}$	$6.82^{+0.07\,+1.70}_{-0.38\,-2.52}$	$12.5 \pm 3.8 \pm 3.1$	–
$\sigma(\psi(2S) + \chi_{c1})$	$0.328^{+0.112}_{-0.097}$	$0.413^{+0.052}_{-0.058}$	$0.566^{+0.004\,+0.123}_{-0.003\,-0.190}$	–	–
$\sigma(\psi(2S) + \chi_{c2})$	$0.420^{+0.144}_{-0.124}$	$0.473^{+0.026}_{-0.048}$	$0.476^{+0.080\,+0.079}_{-0.105\,-0.14}$	–	–
$\sigma(\psi(2S) + \chi_{c1}) + \sigma(\psi(2S) + \chi_{c2})$	$0.75^{+0.26}_{-0.22}$	$0.89^{+0.08}_{-0.11}$	$1.04^{+0.08\,+0.20}_{-0.11\,-0.33}$	<8.6 at 90% C.L.	–

μ_R Dependence

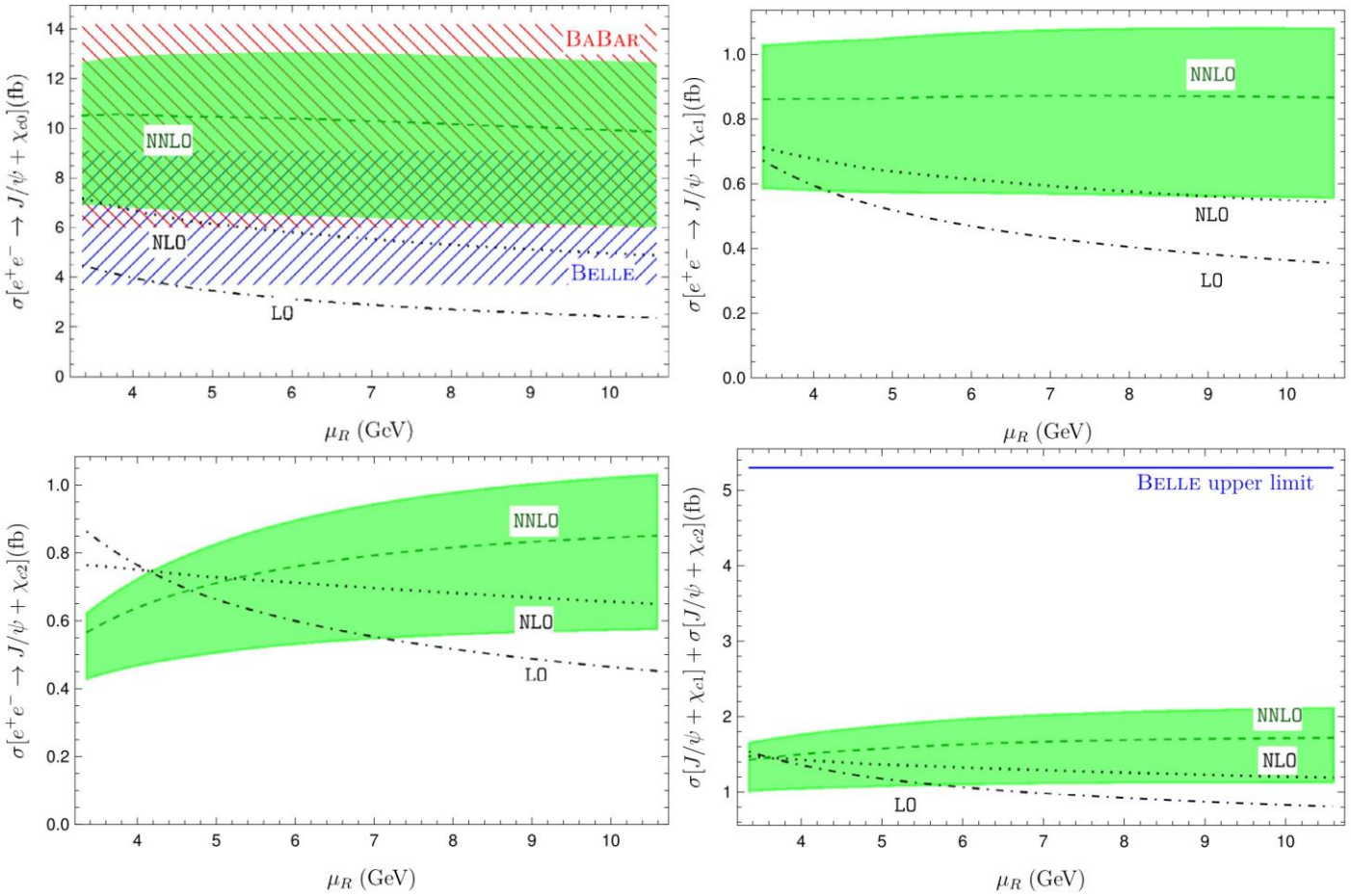

Angular Distribution Parameter

Angular distribution parameter α_J:

$$\frac{\mathrm{d}\sigma(e^+e^- \to J/\psi + \chi_{cJ})}{\mathrm{d}\cos\theta} = A_J\left(1 + \alpha_J \cos^2\theta\right), \qquad J = 0, 1, 2$$

NRQCD predictions for the angular distribution parameter αJ (defined before) at various perturbative accuracy.

	LO	NLO	NNLO	Belle
$J/\psi + \chi_{c0}$	0.252	$0.260^{+0.005}_{-0.004}$	$0.291^{+0.014+0.002}_{-0.012-0.002}$	$-1.01^{+0.38}_{-0.33}$
$J/\psi + \chi_{c1}$	0.697	$0.739^{+0.028}_{-0.027}$	$0.880^{+0.054+0.004}_{-0.060-0.008}$	–
$J/\psi + \chi_{c2}$	−0.197	$-0.075^{+0.012}_{-0.014}$	$0.025^{+0.070+0.005}_{-0.047-0.006}$	–

Optimized correction to exclusive double J/ψ production at B factories

TABLE I. Summary of the signal yields (N), charmonium masses (M), significances, and cross sections ($\sigma_{\rm Born} \times \mathcal{B}_{>2}[(c\bar{c})_{\rm res}]$) for $e^+e^- \to J/\psi(c\bar{c})_{\rm res}$; $\mathcal{B}_{>2}$ denotes the branching fraction for final states with more than two charged tracks.

$(c\bar{c})_{\rm res}$	N	M [GeV/c^2]	Signif.	$\sigma_{\rm Born} \times \mathcal{B}_{>2}$ [fb]
η_c	235 ± 26	2.972 ± 0.007	10.7	$25.6 \pm 2.8 \pm 3.4$
J/ψ	-14 ± 20	fixed	···	<9.1 at 90% CL
χ_{c0}	89 ± 24	3.407 ± 0.011	3.8	$6.4 \pm 1.7 \pm 1.0$
$\chi_{c1} + \chi_{c2}$	10 ± 27	fixed	···	<5.3 at 90% CL
$\eta_c(2S)$	164 ± 30	3.630 ± 0.008	6.0	$16.5 \pm 3.0 \pm 2.4$
$\psi(2S)$	-26 ± 29	fixed	···	<13.3 at 90% CL

TABLE III. Summary of the signal yields (N), significances, and cross sections ($\sigma_{\rm Born} \times \mathcal{B}_{>0}[(c\bar{c})_{\rm res}]$) for $e^+e^- \to \psi(2S) \times (c\bar{c})_{\rm res}$; $\mathcal{B}_{>0}$ denotes the branching fraction for final states containing charged tracks.

$(c\bar{c})_{\rm res}$	N	Signif.	$\sigma_{\rm Born} \times \mathcal{B}_{>0}$ [fb]
η_c	36.7 ± 10.4	4.2	$16.3 \pm 4.6 \pm 3.9$
J/ψ	6.9 ± 8.9	···	<16.9 at 90% CL
χ_{c0}	35.4 ± 10.7	3.5	$12.5 \pm 3.8 \pm 3.1$
$\chi_{c1} + \chi_{c2}$	6.6 ± 8.0	···	<8.6 at 90% CL
$\eta_c(2S)$	36.0 ± 11.4	3.4	$16.0 \pm 5.1 \pm 3.8$
$\psi(2S)$	-8.3 ± 8.5	···	<5.2 at 90% CL

PRD 2008, Belle Collaboration: No evidence for $e^+e^- \to J/\psi J/\psi$!

Double photon fragmentation mechanism

Davier, Peskin and Snynder, 2006 (VMD approach)

FIG. 1: Illustration of the $e^+e^- \to J/\psi + J/\psi$ process through two photon independent fragmentation.

$$\frac{d\sigma_{\rm fr}(e^+e^- \to J/\psi J/\psi)}{d\cos\theta} \approx \left(\frac{ee_c f_{J/\psi}}{M_{J/\psi}}\right)^4 \frac{d\sigma(e^+e^- \to \gamma\gamma)}{d\cos\theta}.$$

Improved NRQCD factorization prediction

The production amplitude can be decomposed to two parts: fragmentation and non-fragmentation pieces

$$\frac{d\sigma}{d\cos\theta} = \frac{1}{2s}\frac{\beta}{16\pi}\frac{1}{4}\sum_{\text{spin}}|\mathcal{M}_{\text{fr}} + \mathcal{M}_{\text{nfr}}|^2$$

While fragmentation piece denotes two photon independent fragmentation into double J/ψ which takes physical J/ψ mass and decay constant as input, non-fragmentation piece is described by traditional NRQCD factorization, expressed in terms of the charm quark mass and J/ψ production long distance matrix element. So the differential cross section can be written as:

$$\frac{d\sigma}{d\cos\theta} = \frac{1}{2s}\frac{\beta}{16\pi}\frac{e^8 e_c^4}{4}\left[\mathcal{C}_{\text{fr}} f_{J/\psi}^4 + \mathcal{C}_{\text{int}} f_{J/\psi}^2 \frac{\langle\mathcal{O}\rangle_{J/\psi}}{m_c} + \mathcal{C}_{\text{nfr}}\left(\frac{\langle\mathcal{O}\rangle_{J/\psi}}{m_c}\right)^2\right]$$

$$\langle\mathcal{O}\rangle_{J/\psi} \equiv |\langle J/\psi(\lambda)|\psi^\dagger \boldsymbol{\sigma}\cdot\boldsymbol{\varepsilon}(\lambda)\chi|0\rangle|^2.$$

Improved NRQCD factorization prediction

$$\frac{d\sigma}{d\cos\theta} = \frac{1}{2s}\frac{\beta}{16\pi}\frac{e^8 e_c^4}{4}\left[\mathcal{C}_{\rm fr} f_{J/\psi}^4 + \mathcal{C}_{\rm int} f_{J/\psi}^2 \frac{\langle\mathcal{O}\rangle_{J/\psi}}{m_c} + \mathcal{C}_{\rm nfr}\left(\frac{\langle\mathcal{O}\rangle_{J/\psi}}{m_c}\right)^2\right]$$

$$\mathcal{C}_{\rm fr} = \frac{8\left(\left(t^2+u^2\right)\left(tu - M_{J/\psi}^4\right) + 4stuM_{J/\psi}^2\right)}{t^2u^2M_{J/\psi}^4}$$

G. T. Bodwin et al. Phys. Rev. D 74, 074014 (2006)

$$\mathcal{C}_{\rm int} = \mathcal{C}_{\rm int}^{(0)}\left[1 + \frac{\alpha_s}{\pi}\hat{c}_{\rm int}^{(1)} + \left(\frac{\alpha_s}{\pi}\right)^2\left(\frac{\beta_0}{4}\ln\frac{\mu_R^2}{m_c^2}\hat{c}_{\rm int}^{(1)} + 2\gamma_{J/\psi}\ln\frac{\mu_\Lambda^2}{m_c^2} + \boxed{\hat{c}_{\rm int}^{(2)}}\right) + \cdots\right]$$

$$\mathcal{C}_{\rm nfr} = \mathcal{C}_{\rm nfr}^{(0)}\left[1 + \frac{\alpha_s}{\pi}\hat{c}_{\rm nfr}^{(1)} + \left(\frac{\alpha_s}{\pi}\right)^2\left(\frac{\beta_0}{4}\ln\frac{\mu_R^2}{m_c^2}\hat{c}_{\rm nfr}^{(1)} + 4\gamma_{J/\psi}\ln\frac{\mu_\Lambda^2}{m_c^2} + \boxed{\hat{c}_{\rm nfr}^{(2)}}\right) + \cdots\right]$$

Two-loop calculation of non-fragmentation piece

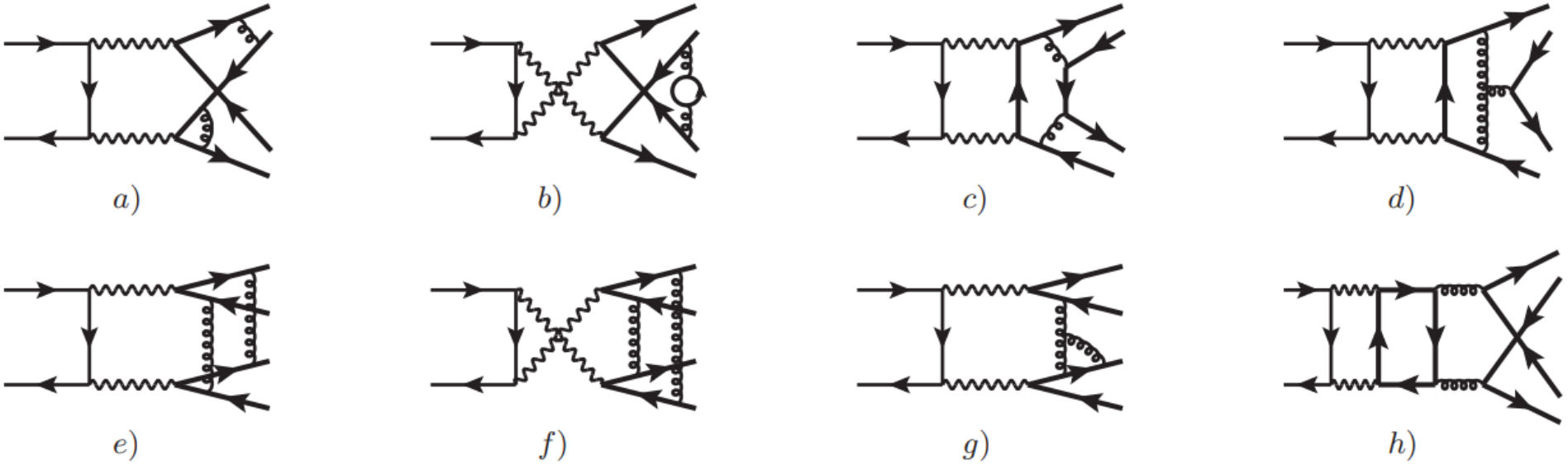

506 two-loop diagrams! —FeynCalc/Formlink, Apart/Fire→ About 2400 master integrals(MIs)

Two-loop 2->4 topology, the cutting-edge calculation

Results of angular distribution of double J/ψ production

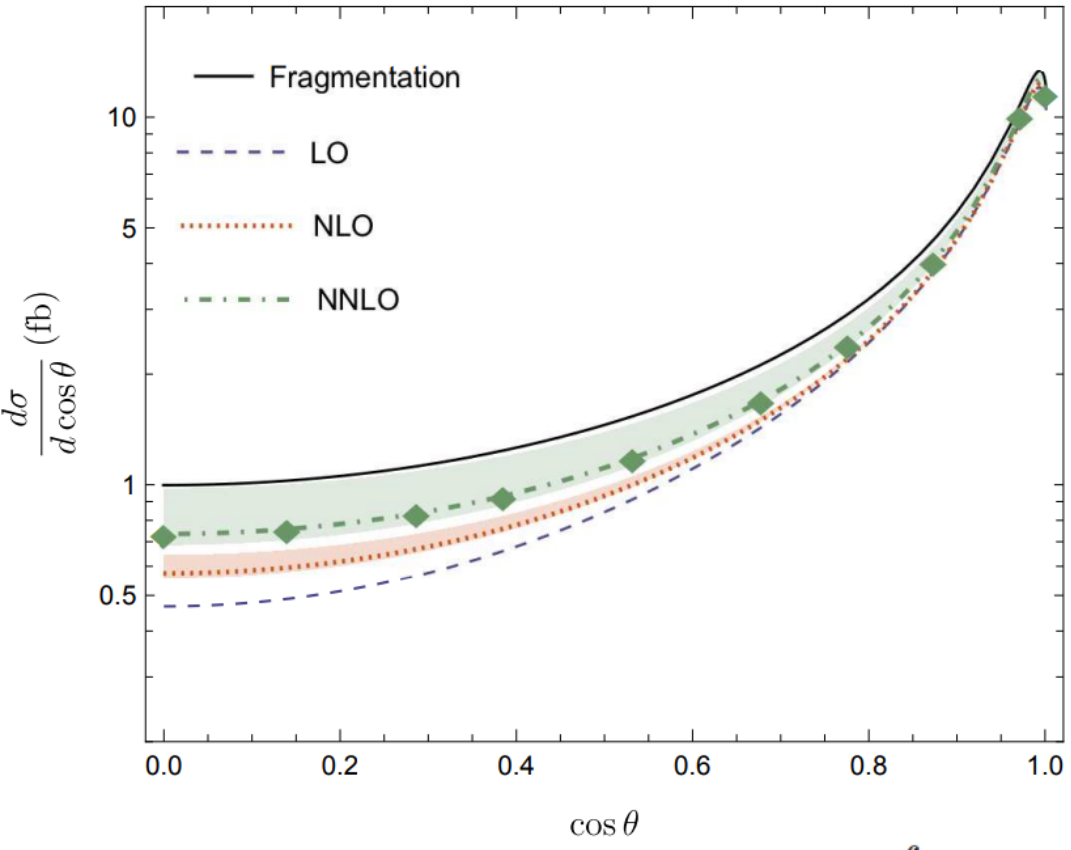

1. Both NLO and NNLO corrections become positive in the improved NRQCD approach;
2. When θ approaches to 0, the fragmentation contribution dominates;
3. When θ deviates from 0, the interference term starts to play some notable role.

$$\langle \mathcal{O} \rangle_{J/\psi}(\mu_\Lambda = 1\ \mathrm{GeV}) = 0.387\ \mathrm{GeV}^3$$

$$\sqrt{s} = 10.58\ \mathrm{GeV} \quad M_{J/\psi} = 3.0969\ \ \mathrm{GeV} \quad f_{J/\psi} = 403\ \mathrm{MeV} \quad m_c = 1.5\ \mathrm{GeV}$$

Band: μ_R range from m_c to $\sqrt{s}$, default value takes at $\sqrt{s}/2$

Compared with Traditional NRQCD factorization prediction

From $$\frac{d\sigma}{d\cos\theta} = \frac{1}{2s}\frac{\beta}{16\pi}\frac{e^8 e_c^4}{4}\left[\mathcal{C}_{\rm fr} f_{J/\psi}^4 + \mathcal{C}_{\rm int} f_{J/\psi}^2 \frac{\langle\mathcal{O}\rangle_{J/\psi}}{m_c} + \mathcal{C}_{\rm nfr}\left(\frac{\langle\mathcal{O}\rangle_{J/\psi}}{m_c}\right)^2\right]$$

Use: $$f_{J/\psi} = \sqrt{\frac{2\langle\mathcal{O}\rangle_{J/\psi}}{M_{J/\psi}}}\left[1 + \mathfrak{f}^{(1)}\frac{\alpha_s}{\pi} + \left(\frac{\alpha_s}{\pi}\right)^2\left(\mathfrak{f}^{(1)}\frac{\beta_0}{4}\ln\frac{\mu_R^2}{m_c^2} + \gamma_{J/\psi}\ln\frac{\mu_\Lambda^2}{m_c^2} + \mathfrak{f}^{(2)}\right) + \cdots\right] + \mathcal{O}(v^2)$$

and

$$\mathcal{C}_{\rm int} = \mathcal{C}_{\rm int}^{(0)}\left[1 + \frac{\alpha_s}{\pi}\hat{c}_{\rm int}^{(1)} + \left(\frac{\alpha_s}{\pi}\right)^2\left(\frac{\beta_0}{4}\ln\frac{\mu_R^2}{m_c^2}\hat{c}_{\rm int}^{(1)} + 2\gamma_{J/\psi}\ln\frac{\mu_\Lambda^2}{m_c^2} + \hat{c}_{\rm int}^{(2)}\right) + \cdots\right]$$

$$\mathcal{C}_{\rm nfr} = \mathcal{C}_{\rm nfr}^{(0)}\left[1 + \frac{\alpha_s}{\pi}\hat{c}_{\rm nfr}^{(1)} + \left(\frac{\alpha_s}{\pi}\right)^2\left(\frac{\beta_0}{4}\ln\frac{\mu_R^2}{m_c^2}\hat{c}_{\rm nfr}^{(1)} + 4\gamma_{J/\psi}\ln\frac{\mu_\Lambda^2}{m_c^2} + \hat{c}_{\rm nfr}^{(2)}\right) + \cdots\right]$$

One can go back to Traditional NRQCD factorization:

$$\frac{d\sigma}{d\cos\theta} = \frac{1}{2s}\frac{\beta}{16\pi}\frac{e^8 e_c^4}{4}\mathcal{F}^{(0)}\left[1 + \frac{\alpha_s}{\pi}f^{(1)} + \left(\frac{\alpha_s}{\pi}\right)^2\left(f^{(1)}\frac{\beta_0}{4}\ln\frac{\mu_R^2}{m_c^2} + 4\gamma_{J/\psi}\ln\frac{\mu_\Lambda^2}{m_c^2} + f^{(2)}\right)\right]\frac{\langle\mathcal{O}\rangle_{J/\psi}^2}{m_c^2}$$

Differential section of double J/ψ production comparison

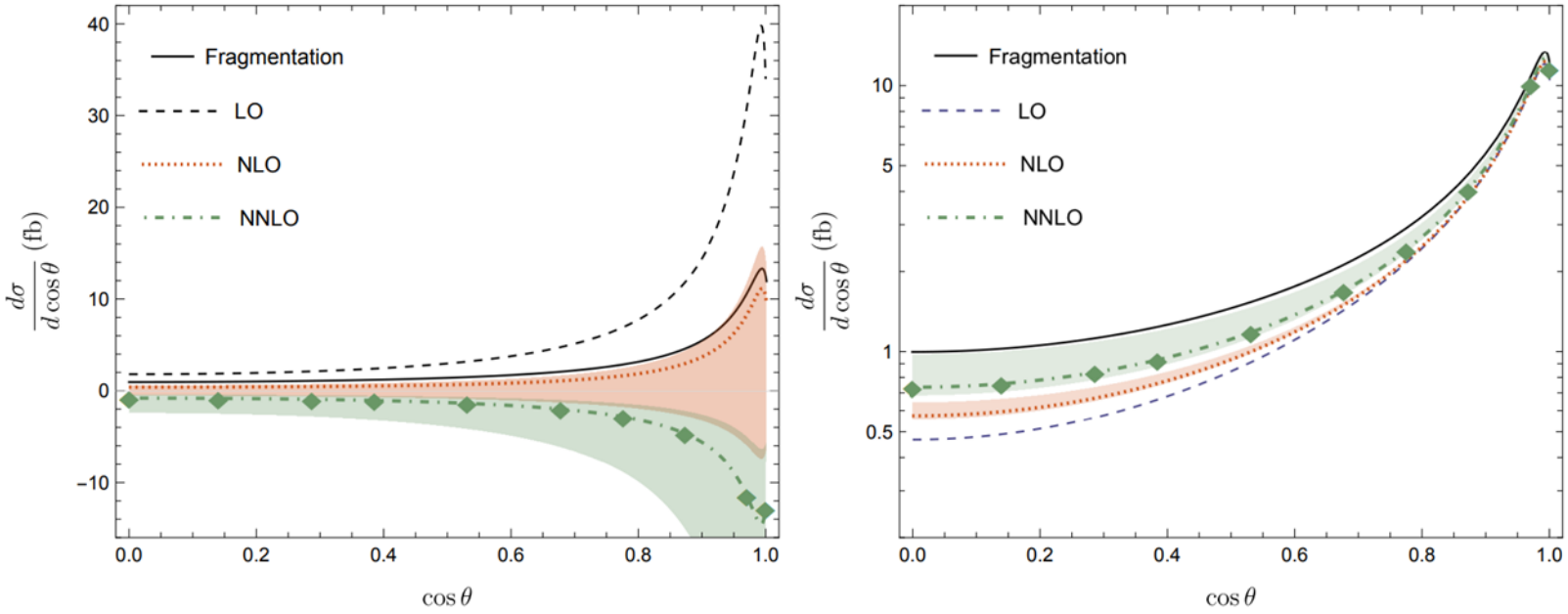

Traditional Optimized

Optimized NRQCD: Positive, exhibit decent convergence behavior and modest renormlization scale dependence!

Predicted total cross section of double J/ψ production from improved and traditional NRQCD factorization

σ (fb)	Fragmentation	LO	NLO	NNLO
Optimized NRQCD	2.52	1.85	$1.93^{+0.05}_{-0.01}$	$2.13^{+0.30}_{-0.06}$
Traditional NRQCD		6.12	$1.56^{+0.73}_{-2.95}$	$-2.38^{+1.27}_{-5.35}$

Optimized NRQCD: Positive and converge decently →
Expect to observe clean signal events at Belle 2

Traditional NRQCD: Unphysical negative total section

Non-trivial validation of NRQCD factorization

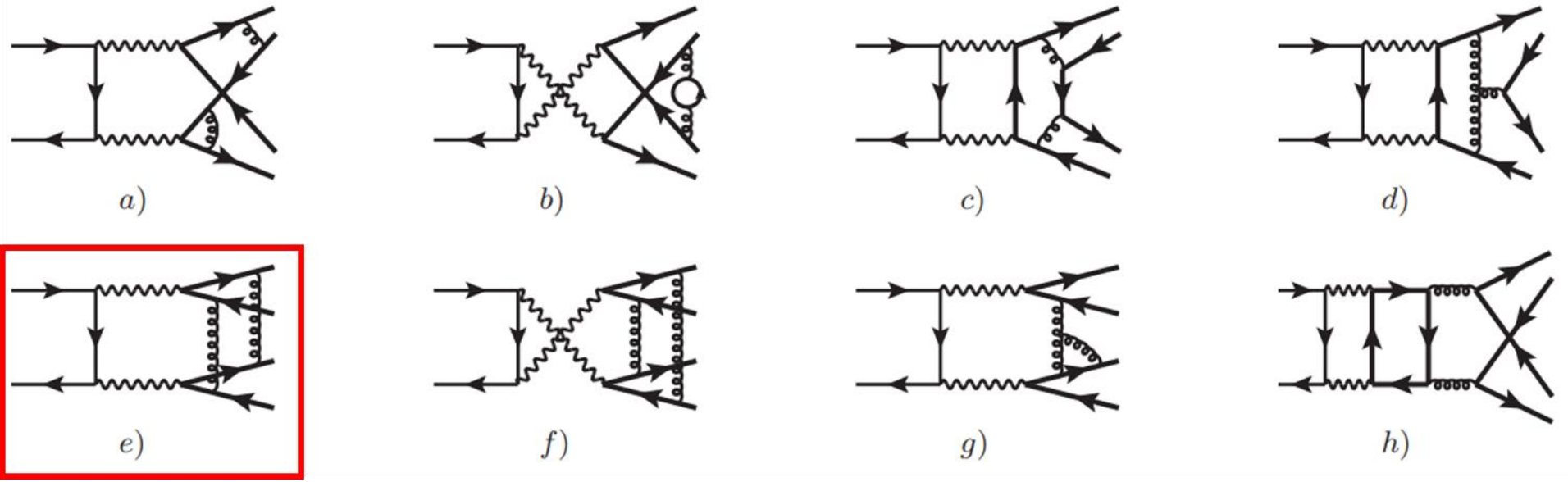

$cos\theta = 0$:$1/\varepsilon_{IR}^2$. Take diagram e) as an example:

$$\mathcal{M}^{\text{Fig.4e)}}\Big|_{\theta=\frac{\pi}{2}} = \frac{1}{\epsilon_{\text{IR}}^2}\frac{C_F\,\alpha^2}{2N_c}\frac{(m_c^2+2\mathbf{P}^2)^2}{16\mathbf{P}^2(4m_c^2+\mathbf{P}^2)}\left(\ln\frac{1+\beta}{1-\beta}-i\pi\right)^2\mathcal{M}_{\text{fr},0}^{\text{Fig.1}a)}\Big|_{\theta=\frac{\pi}{2}}+\mathcal{O}(1/\epsilon_{\text{IR}})$$

$|\mathbf{P}|$ denotes the magnitude of the J/ψ momentum

B8. Heavy quarkonium production and decay

Work 3: Three-loop QCD corrections to quarkonium electroweak decay

F. Feng, **Y. J.**, Z. Mo, J. Pan, W. L. Sang and J. Y. Zhang, Complete three-loop QCD corrections to leptonic width of vector quarkonium. [arXiv:2207.14259 [hep-ph]].

F. Feng, **Y. J.**, Z. W. Mo, J. C. Pan and W. L. Sang , Three-loop QCD corrections to the decay constant of B_c. [arXiv:2208.04302 [hep-ph]].

J/psi and Upsilon leptonic widths measured very precisely

$J/\psi(1S)$ DECAY MODES		Fraction (Γ_i/Γ)	Scale factor/ Confidence level	p (MeV/c)
hadrons		(87.7 ± 0.5) %		–
virtual $\gamma \rightarrow$ hadrons		(13.50 ± 0.30) %		–
ggg		(64.1 ± 1.0) %		–
γgg		(8.8 ± 1.1) %		–
e^+e^-		(5.971 ± 0.032) %		1548
$e^+e^-\gamma$	[a]	(8.8 ± 1.4) $\times 10^{-3}$		1548

Leptonic decay of quarkonia is one of the most important and clean channel to reconstruct quarkonia.

Vector quarkoniumn leptonic decay: NRQCD description

Decay rate

$$\Gamma(V \to l^+ l^-) = \frac{4\pi\alpha^2}{3M_V}|f_V|^2$$

$$\langle 0|\mathcal{J}^\mu_{\mathrm{EM}}|\,V(\boldsymbol{\epsilon})\rangle = M_V f_V \epsilon^\mu_V, \quad \mathcal{J}^\mu_{\mathrm{EM}} = \sum_f e_f \bar{\Psi}_f \gamma^\mu \Psi_f$$

The leptonic decay constants can be calculated via NRQCD factorization

$$\begin{aligned}\langle 0|\mathcal{J}^i_{\mathrm{EM}}|\,V(\epsilon)\rangle =& \sqrt{2M_V}e_Q\mathcal{C}_0\langle 0|\chi^\dagger\sigma^i\psi|\,V(\epsilon)\rangle_{\mathrm{NR}} + \mathcal{O}(v^2)\\ =& \sqrt{2M_V}e_Q\left(\mathcal{C}_{\mathrm{dir}} + \sum_{f\neq Q}\mathcal{C}_{\mathrm{ind,f}}\frac{e_f}{e_Q}\right)\langle 0|\chi^\dagger\sigma^i\psi|\,V(\epsilon)\rangle_{\mathrm{NR}} + \mathcal{O}(v^2)\end{aligned}$$

NRQCD factorization

$$\mathcal{C}_0\left(\frac{\mu_R}{m_Q},\frac{\mu_\Lambda}{m_Q},x\right)=$$
$$1+\frac{\alpha_s(\mu_R)}{\pi}\mathcal{C}^{(1)}(x)+\left(\frac{\alpha_s(\mu_R)}{\pi}\right)^2\left[\mathcal{C}^{(1)}\frac{\beta_0}{4}\ln\frac{\mu_R^2}{m_Q^2}+\gamma^{(2)}\ln\frac{\mu_\Lambda^2}{m_Q^2}+\mathcal{C}^{(2)}(x)\right]$$
$$+\left(\frac{\alpha_s(\mu_R)}{\pi}\right)^3\left\{\frac{\mathcal{C}^{(1)}}{16}\beta_0^2\ln^2\frac{\mu_R^2}{m_Q^2}+\left[\frac{\mathcal{C}^{(1)}}{16}\beta_1+\mathcal{C}^{(2)}(x)\frac{\beta_0}{2}\right]\ln\frac{\mu_R^2}{m_Q^2}\right.$$
$$+\gamma^{(2)}\frac{\beta_0}{2}\ln\frac{\mu_\Lambda^2}{m_Q^2}\ln\frac{\mu_R^2}{m_Q^2}+\frac{1}{4}\left[2\frac{\mathrm{d}\gamma^{(3)}(\mu_\Lambda)}{\mathrm{d}\ln\mu_\Lambda^2}-\beta_0\gamma^{(2)}\right]\ln^2\frac{\mu_\Lambda^2}{m_Q^2}$$
$$\left.+\left[\mathcal{C}^{(1)}\gamma^{(2)}+\gamma^{(3)}(m_Q)\right]\ln\frac{\mu_\Lambda^2}{m_Q^2}+\mathcal{C}^{(3)}(x)\right\}+\mathcal{O}\left(\alpha_s^4\right).$$

$$x:=\frac{m_M}{m_H}$$

m_M: Mass of intermediate quark

m_H: Mass of external leg quark

$C^{(1)}(x)$:Barbieri, R. Gatto, et al., PLB1975; Celmaster, PRD1979

$C^{(2)}(x)$:Beneke, Signer, Smirnov, PRL1998; Czarnecki, Melniko, PRL1998; Kniehl, Onishchenko, et al., PLB2006; Egner, Fael, et al., PRD2021

$C^{(3)}(x)$ without charm mass effect and indirect term: Marquard, Piclum, et al., NPB2006, PLB2009, PRD2014; Beneke, Kiyo, et al., PRL2014

About 300 diagrams !

Feynman Diagrams

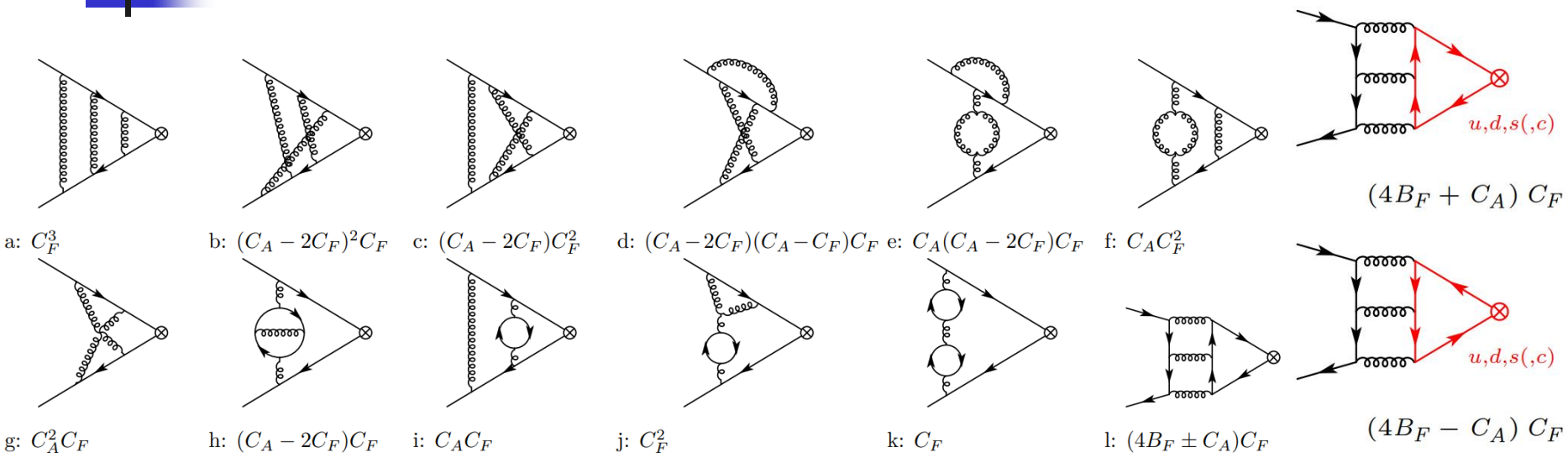

Representative diagrams for the direct channel. B_F is defined as $\sum_{bc} d^{abc}d^{ebc} \equiv 4B_F\delta^{ae}$ and $B_F = (N_c^2-4)/(4N_c)$ for the $SU(N_c)$.

Indirect diagrams

$$\mathcal{C}_{\rm dir}^{(3)} = C_F\Big[C_F^2\mathcal{C}_{FFF} + C_FC_A\mathcal{C}_{FFA} + C_A^2\mathcal{C}_{FAA}$$
$$+ T_Fn_L\left(C_F\mathcal{C}_{FFL} + C_A\mathcal{C}_{FAL} + T_Fn_H\mathcal{C}_{FHL} + T_Fn_M\mathcal{C}_{FML}(x) + T_Fn_L\mathcal{C}_{FLL}\right)$$
$$+ T_Fn_H\left(C_F\mathcal{C}_{FFH} + C_A\mathcal{C}_{FAH} + T_Fn_H\mathcal{C}_{FHH} + T_Fn_M\mathcal{C}_{FHM}(x) + B_F\mathcal{C}_{BFH}\right)$$
$$+ T_Fn_M\left(C_F\mathcal{C}_{FFM}(x) + C_A\mathcal{C}_{FAM}(x) + T_Fn_M\mathcal{C}_{FMM}(x)\right)\Big]$$

Red term: charm mass effect

Three-loop Anomalous Dimension of NRQCD vector current

New piece of three loop anomalous dimension of vector current in NRQCD reconstructed by utilizing Thiele's interpolation formula and PSLQ algorithm

$$\gamma_v = -\frac{\mathrm{d}\ln\langle\mathcal{O}_v\rangle}{\mathrm{d}\ln\mu_\Lambda^2} = -\left(\frac{\alpha_s}{\pi}\right)^2\gamma_v^{(2)} - \left(\frac{\alpha_s}{\pi}\right)^3\gamma_v^{(3)}(\mu_\Lambda) \quad \mathcal{O}_v = \chi^\dagger\boldsymbol{\sigma}\cdot\boldsymbol{\varepsilon}\psi$$

$$\gamma_v^{(2)} = -3\pi^2 C_F\left(\frac{1}{18}C_F + \frac{1}{12}C_A\right),$$

$$\begin{aligned}\gamma_v^{(3)}(\mu_\Lambda) = -3\pi^2 C_F\Bigg\{ &\left(\frac{43}{144} - \frac{1}{2}\ln 2\right)C_F^2 + \left(\frac{113}{324} + \frac{1}{4}\ln 2\right)C_F C_A + \left(\frac{2}{27} + \frac{1}{4}\ln 2\right)C_A^2 \\ &+ T_F n_L\left(-\frac{25}{324}C_F - \frac{37}{432}C_A\right) + \frac{1}{60}T_F n_H C_F \\ &+ T_F n_M\left[\frac{C_F}{60x^2} + \left(\frac{1}{18}C_F + \frac{1}{12}C_A\right)\ln x^2\right] + \ln\frac{\mu_\Lambda^2}{m_Q^2}\left[\frac{5}{48}C_F^2 + \frac{5}{32}C_F C_A\right. \\ &\left. + \frac{1}{24}C_A^2 - T_F n_M\left(\frac{1}{18}C_F + \frac{1}{12}C_A\right)\right]\Bigg\}. \end{aligned} \tag{12}$$

SDCs (with the aid of AMFlow)

$$\mathcal{C}_{FFF} = 36.4948624588059253763347618987279203166418 1$$

$$\mathcal{C}_{FFA} = -188.0778416598807139057999402327847645038910 5$$

$$\mathcal{C}_{FAA} = -97.7349732699183863423452450045740984398871 81$$

$$\mathcal{C}_{FFL} = 46.6916929055151324675582676412605360177791267 74$$

$$\mathcal{C}_{FAL} = 39.6237185545244190773420474220534775186981204767$$

$$\mathcal{C}_{FHL} = -0.270250439156502171732138691397778647923997721,$$

$$\mathcal{C}_{FLL} = -2.468336454482374116370541876524861896589683 86,$$

$$\mathcal{C}_{FFH} = -0.843562291159500145305509373641959358579825 2$$

$$\mathcal{C}_{FAH} = -0.102474161492931740857483597199380212016310 6$$

$$\mathcal{C}_{FHH} = 0.051239607511983724934931185889964136984463561 7,$$

$$\mathcal{C}_{BFH} = 2.115578267980906498436822221913944370044335 6 + \mathrm{i}\, 0.4942127107006720402412181080201603811552204 87),$$

$$\mathcal{C}^{(3)}_{\mathrm{ind},l} = T_F B_F C_F(-0.945532642977386 + \mathrm{i}\, 1.28500237447426).$$

For terms free from charm mass effect(independent of x), we confirm the results(black numbers) from Egner, Fael, et al. arXiv:2203.11231 and achieve high precision

SDCs (include finite charm mass and singlet contributions)

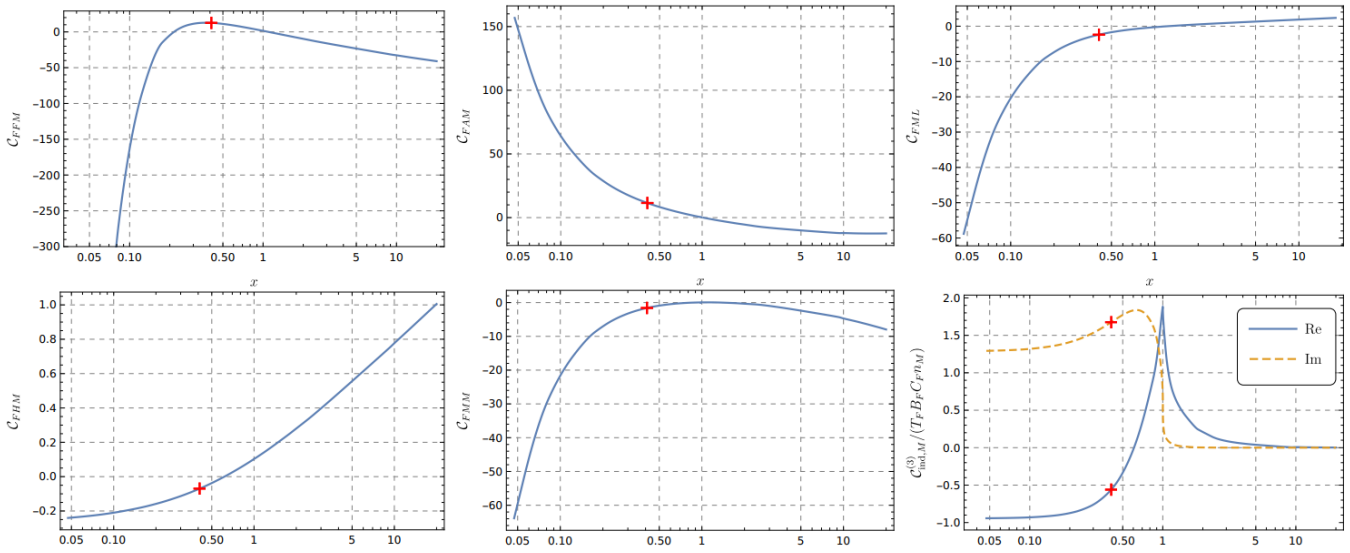

For terms dependent of x, we draw the diagram of SDC-x. Red crosses are the physical values with three-loop pole masses of quarks m_Q ≡ m_b = 4.98 GeV, m_M ≡ m_c = 2.04 GeV(RunDec from $m_c(m_c)$ = 1.28GeV, $m_b(m_b)$ = 4.18GeV)

Phenomenological analysis: a disaster

$\Gamma(\mathrm{keV})$ / V	LO	NLO	NNLO	N^{3}LO			PDG
				Direct ($m_M = 0$)	Direct ($m_M \neq 0$)	Total	
Υ	1.6529	$1.0556^{+0.1063}_{-0.3838}$	$0.9400^{+0.0647}_{-0.0570}$	$-0.4304^{+0.6238}_{-4.5256}$	$-0.4887^{+0.6551}_{-4.8010}$	$-0.4884^{+0.6549}_{-4.7999}$	1.340 ± 0.018
J/ψ	4.8392	$2.3901^{+0.6318}_{-1.5593}$	$0.5135^{+1.0758}_{-2.7118}$	$-11.8733^{+7.8098}_{-40.0618}$			5.53 ± 0.10

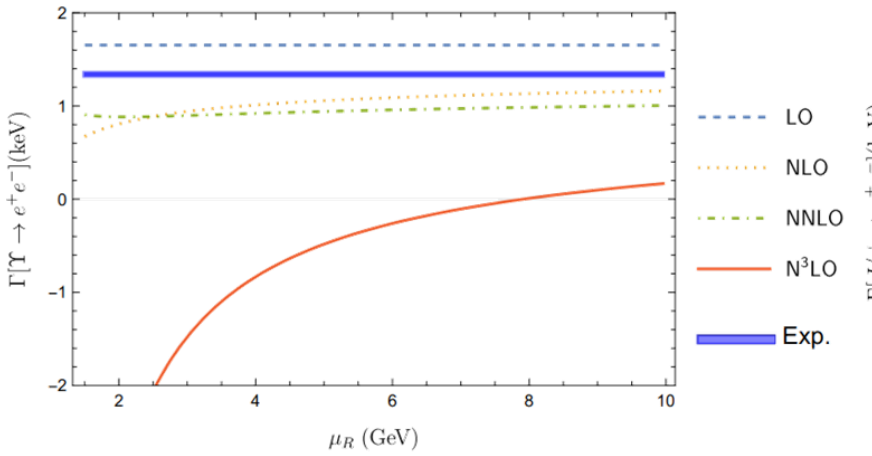

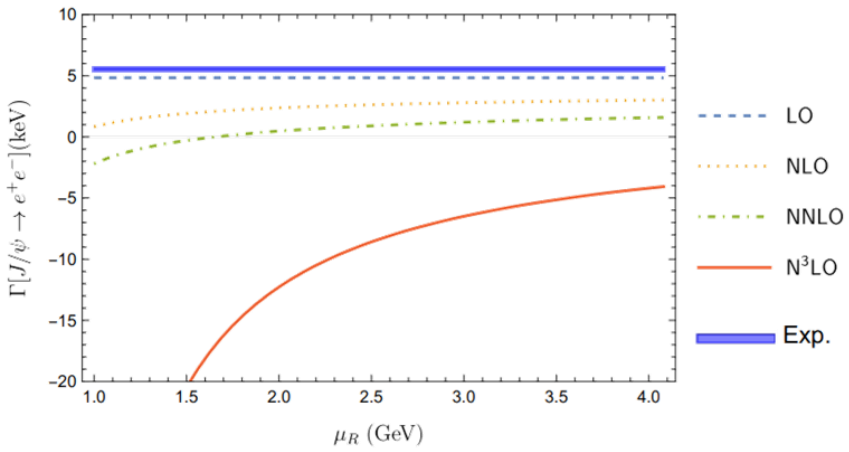

Phenomenological analysis

Phenomenological analysis: charm mass effect and indirect term effect

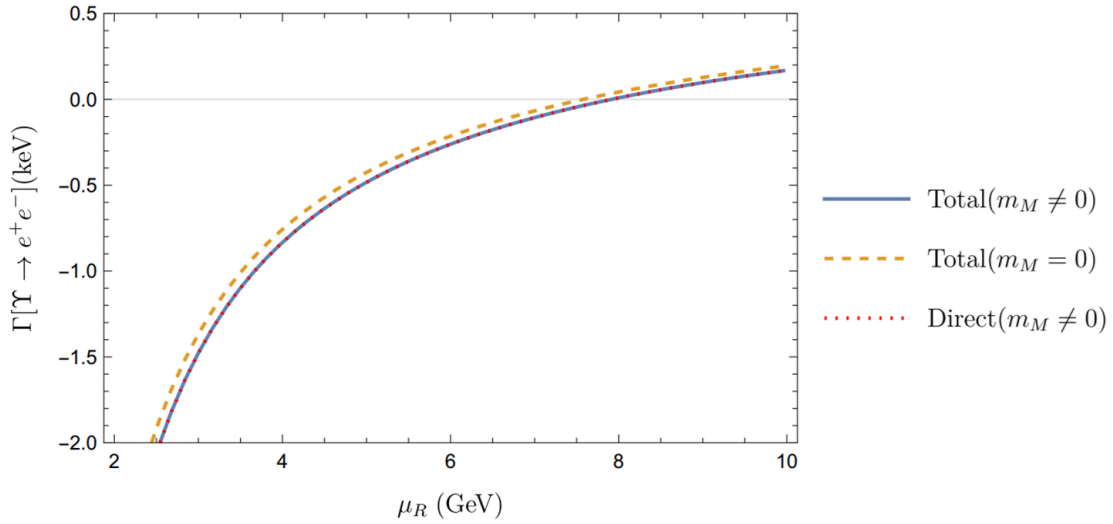

It’s shown that indirect channel only has invisible effect on the plot, while charm mass leads to visible small correction

Bc decay to lepton and neutrino

Decay rate

$$\Gamma\left(B_c \to l^+ \nu_l\right) = \frac{1}{8\pi} |V_{bc}|^2 G_F^2 M_{B_c} m_l^2 \left(1 - \frac{m_l^2}{M_{B_c}^2}\right)^2 f_{B_c}^2$$

The decay constants can be calculated via NRQCD factorization

$$\begin{aligned}\langle 0|\bar{b}\gamma^\mu\gamma_5 c|B_c^+(P)\rangle =& \mathrm{i}P^\mu f_{B_c} \\ =& \sqrt{2M_{B_c}}\mathcal{C}_0(x)\langle 0|\chi_b^\dagger \psi_c|B_c^+\rangle_{\mathrm{NR}} + \mathcal{O}\left(v^2\right) \quad x = \frac{m_c}{m_b}\end{aligned}$$

Bc decay: 3-loop Diagrams

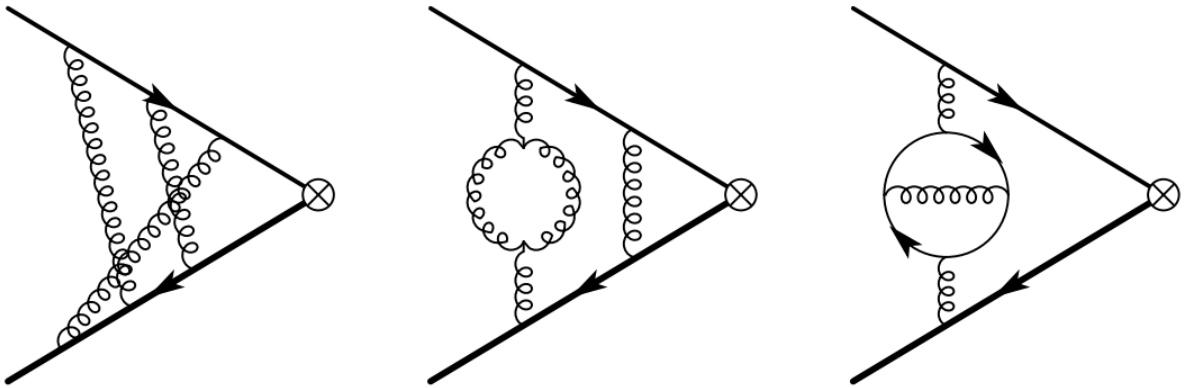

Typical Feynman diagrams for $c\bar{b} \to W$ at three-loop order.

$$
\begin{aligned}
\mathcal{C}_0(x) = & C_F \big[C_F^2 \mathcal{C}_{FFF} + C_F C_A \mathcal{C}_{FFA} + C_A^2 \mathcal{C}_{FAA} \\
& + T_F n_L \left(C_F \mathcal{C}_{FFL} + C_A \mathcal{C}_{FAL} + T_F n_H \mathcal{C}_{FHL} + T_F n_M \mathcal{C}_{FML} + T_F n_L \mathcal{C}_{FLL} \right) \\
& + T_F n_H \left(C_F \mathcal{C}_{FFH} + C_A \mathcal{C}_{FAH} + T_F n_H \mathcal{C}_{FHH} + T_F n_M \mathcal{C}_{FHM} + B_F \mathcal{C}_{BFH} \right) \\
& + T_F n_M \left(C_F \mathcal{C}_{FFM} + C_A \mathcal{C}_{FAM} + T_F n_M \mathcal{C}_{FMM} \right) \big].
\end{aligned}
$$

Anomalous Dimension

Totally new three loop anomalous dimension of pseudoscalar current consisting of different heavy flavor quark in NRQCD reconstructed by utilizing Thiele’ s interpolation formula and PSLQ algorithm .

$$\gamma_p = -\frac{\mathrm{d}\ln\langle\mathcal{O}_p\rangle}{\mathrm{d}\ln\mu_\Lambda^2} = -\left(\frac{\alpha_s}{\pi}\right)^2\gamma_p^{(2)} - \left(\frac{\alpha_s}{\pi}\right)^3\gamma_p^{(3)}(\mu_\Lambda) \quad ,\mathcal{O}_p = \chi_b^\dagger\psi_c$$

$$\gamma^{(3)}\left(x,\frac{\mu_\Lambda^2}{m_M^2}\right) = -\pi^2 C_F\left[\left(\frac{29+38z}{24\,(1+z)} - \frac{7}{4}\ln 2 - \frac{2-3x-22x^2-3x^3+2x^4}{4\,(1-x)\,(1+x)^3}\ln x + \frac{1}{4}\ln(1+z)\right.\right.$$
$$\left.+\frac{-1+6z}{8\,(1+z)}\ln\frac{\mu_\Lambda^2}{m_M^2}\right)C_F^2 + \left(\frac{93+52z}{72\,(1+z)} + \frac{3}{8}\ln 2 - \frac{5+2x+5x^2}{16\,(1-x)\,(1+x)}\ln x + \frac{3}{8}\ln(1+z)\right.$$
$$\left.+\frac{18+11z}{16\,(1+z)}\ln\frac{\mu_\Lambda^2}{m_M^2}\right)C_F C_A + \left(\frac{2}{9} + \frac{5}{8}\ln 2 + \frac{1}{8}\ln(1+z) + \frac{1}{8}\ln\frac{\mu_\Lambda^2}{m_M^2}\right)C_A^2$$
$$\left.- T_F n_l\left(\frac{15+7z}{36\,(1+z)}C_F + \frac{37}{144}C_A\right) + T_F n_b\frac{1}{5\,(1+1/x)^2}C_F + T_F n_c\frac{1}{5\,(1+x)^2}C_F\right].$$

Three-loop SDCs

High precision of SDC and diagrams of SDC-mass ratio obtained!

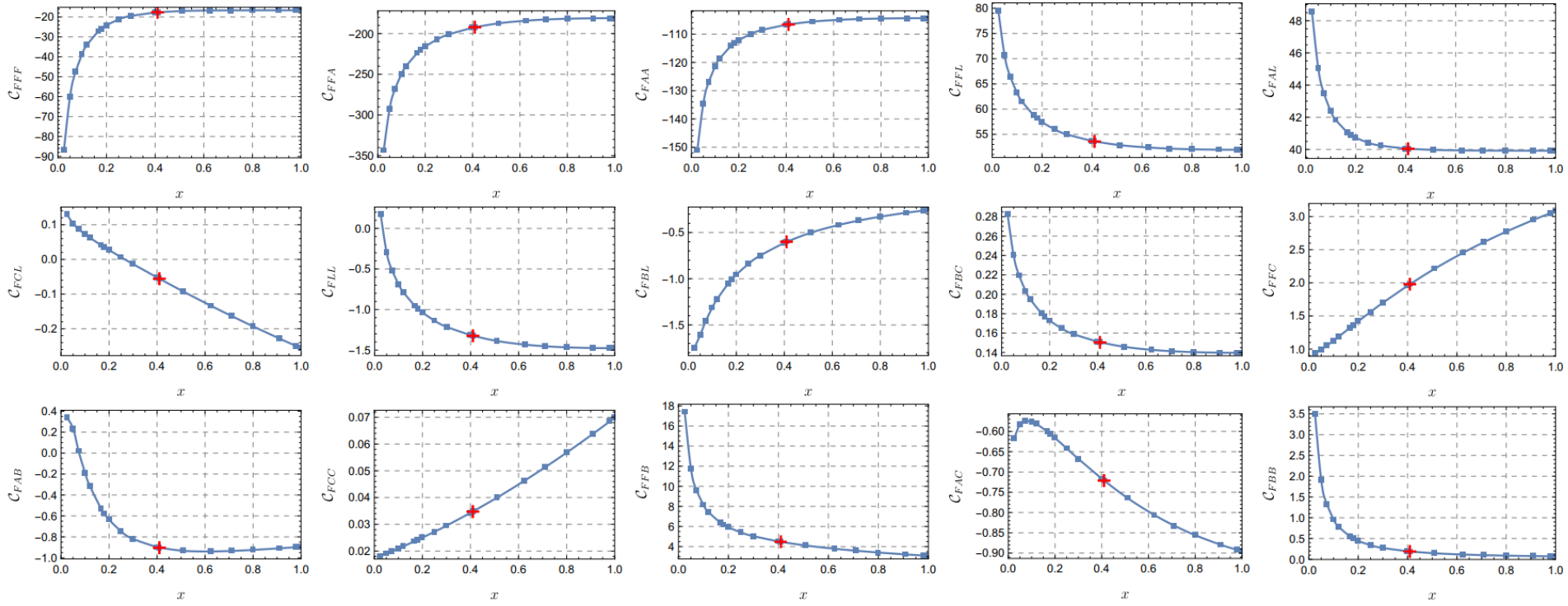

Phenomenological analysis: a disaster

	LO	NLO	NNLO	$\mathrm{N^3LO}$
leptonic width($\times 10^{-7}$ eV)	1.4776	$0.9207^{+0.1848}_{-0.1895}$	$0.7148^{+0.1965}_{-0.1606}$	$-6.2285^{+4.9766}_{-9.7396}$
$\mathcal{B}(B_c \to \mu^+ + \nu_\mu)$ $(\times 10^{-4})$	1.1449	$0.7134^{+0.1432}_{-0.1468}$	$0.5539^{+0.1522}_{-0.1245}$	$-4.8260^{+3.8560}_{-7.5465}$

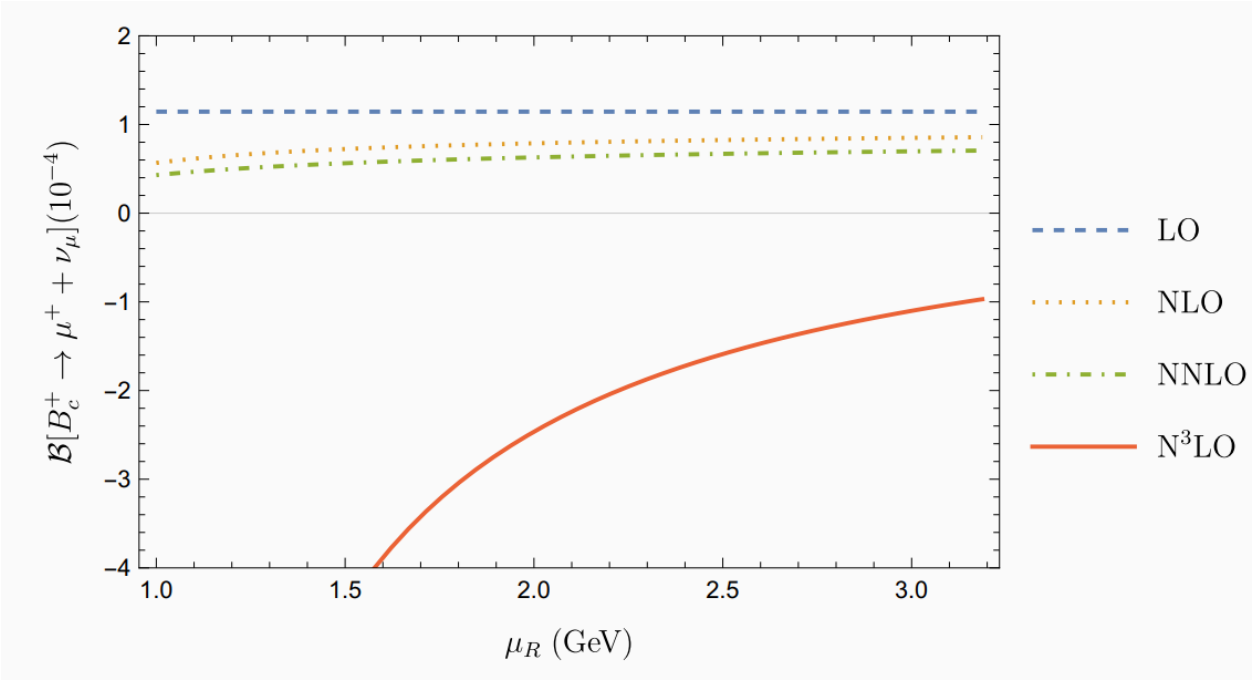

Branching ratio of the Bc weak decay

End with a small project for fun: marginally linked with A3+B8

Work 4: Soft pattern of Rutherford scattering from heavy target mass expansion

Y. J. and J.-Y. Zhang, Soft pattern of Rutherford scattering from heavy target mass expansion, 2303.18243, to appear in Chinese Physics C

Soft pattern of Rutherford scattering from heavy target mass expansion

- 1909: Geiger & Marsden : gold foil experiment
- **1911: Rutherford formula: introduce the concept of atomic nucleus**
- The exchanged photon carries long wavelength and can not deeply probe the internal structure of the composite target.
- Gell-Mann and Low studied the soft limit of the angular distribution of the Compton scattering in the 1950.

- We are going to investigate the low-energy limit of Rutherford scattering

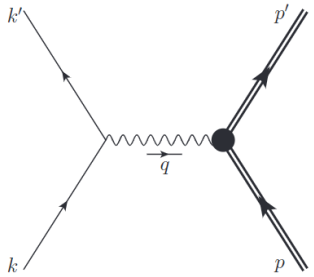

EM Form Factors for composite target carrying various spins (from 0 to 2)

$$\langle N(p',\lambda')|J^{\mu}|N(p,\lambda)\rangle_{s=0} = 2P^{\mu}F_{1,0}\left(\frac{q^2}{M^2}\right),$$

$$\langle N(p',\lambda')|J^{\mu}|N(p,\lambda)\rangle_{s=\frac{1}{2}} = \bar{u}(p',\lambda')\left[2P^{\mu}F_{1,0}\left(\frac{q^2}{M^2}\right) + i\sigma^{\mu\nu}q_{\nu}F_{2,0}\left(\frac{q^2}{M^2}\right)\right]u(p,\lambda),$$

$$\begin{aligned}\langle N(p',\lambda')|J^{\mu}|N(p,\lambda)\rangle_{s=1} = &-\varepsilon^{*}_{\alpha'}(p',\lambda')\Bigg\{2P^{\mu}\left[g^{\alpha'\alpha}F_{1,0}\left(\frac{q^2}{M^2}\right) - \frac{q^{\alpha'}q^{\alpha}}{2M^2}F_{1,1}\left(\frac{q^2}{M^2}\right)\right]\\ &-\left(g^{\mu\alpha'}q^{\alpha} - g^{\mu\alpha}q^{\alpha'}\right)F_{2,0}\left(\frac{q^2}{M^2}\right)\Bigg\}\varepsilon_{\alpha}(p,\lambda),\end{aligned}$$

$$\begin{aligned}\langle N(p',\lambda')|J^{\mu}|N(p,\lambda)\rangle_{s=\frac{3}{2}} = &-\bar{u}_{\alpha'}(p',\lambda')\Bigg\{2P^{\mu}\left[g^{\alpha'\alpha}F_{1,0}\left(\frac{q^2}{M^2}\right) - \frac{q^{\alpha'}q^{\alpha}}{2M^2}F_{1,1}\left(\frac{q^2}{M^2}\right)\right]\\ &+ i\sigma^{\mu\nu}q_{\nu}\left[g^{\alpha'\alpha}F_{2,0}\left(\frac{q^2}{M^2}\right) - \frac{q^{\alpha'}q^{\alpha}}{2M^2}F_{2,1}\left(\frac{q^2}{M^2}\right)\right]\Bigg\}u_{\alpha}(p,\lambda),\end{aligned}$$

$$\begin{aligned}\langle N(p',\lambda')|J^{\mu}|N(p,\lambda)\rangle_{s=2} = &\varepsilon^{*}_{\alpha'_1\alpha'_2}(p',\lambda')\Bigg\{2P^{\mu}\Bigg[g^{\alpha'_1\alpha_1}g^{\alpha'_2\alpha_2}F_{1,0}\left(\frac{q^2}{M^2}\right) - \frac{q^{\alpha'_1}q^{\alpha_1}}{2M^2}g^{\alpha'_2\alpha_2}F_{1,1}\left(\frac{q^2}{M^2}\right)\\ &+ \frac{q^{\alpha'_1}q^{\alpha_1}}{2M^2}\frac{q^{\alpha'_2}q^{\alpha_2}}{2M^2}F_{1,2}\left(\frac{q^2}{M^2}\right)\Bigg] - \left(g^{\mu\alpha'_2}q^{\alpha_2} - g^{\mu\alpha_2}q^{\alpha'_2}\right)\\ &\times\left[g^{\alpha'_1\alpha_1}F_{2,0}\left(\frac{q^2}{M^2}\right) - \frac{q^{\alpha'_1}q^{\alpha_1}}{2M^2}F_{2,1}\left(\frac{q^2}{M^2}\right)\right]\Bigg\}\varepsilon_{\alpha_1\alpha_2}(p,\lambda).\end{aligned}$$

$F_{1,0}(0)=Z$: total electric charge in units of e

$F_{1,0}(0)+F_{1,1}(0)$:the electric quadrupole moment in units of e/(2M)

$F_{2,0}(0)$: magnetic dipole moment in units of e/M^2

$F_{2,0}(0)+F_{2,1}(0)$: magnetic octupole moment in units of e/(2M^3)

low-energy spin-1/2 massless projectile

$$\frac{\mathrm{d}\sigma}{\mathrm{d}\cos\theta} = \frac{\pi\alpha^2 Z^2 \cos^2\frac{\theta}{2}}{2\mathbf{k}^2 \sin^4\left(\frac{\theta}{2}\right)} - \frac{\pi\alpha^2 Z^2 \cos^2\frac{\theta}{2}}{M|\mathbf{k}|\sin^2\left(\frac{\theta}{2}\right)} + \mathcal{O}\left(\frac{1}{M^2}\right)$$

$$\left(\frac{\mathrm{d}\sigma}{\mathrm{d}\cos\theta}\right)^{s=0}_{\mathrm{NNLO}} = -\frac{4\pi\alpha^2}{M^2\sin^2\frac{\theta}{2}}\left(F'_{1,0}Z\cos^2\frac{\theta}{2} + \frac{1}{8}Z^2\cos^2\theta - \frac{1}{8}Z^2\right)$$

$$\left(\frac{\mathrm{d}\sigma}{\mathrm{d}\cos\theta}\right)^{s=\frac{1}{2}}_{\mathrm{NNLO}} = -\frac{4\pi\alpha^2}{M^2\sin^2\frac{\theta}{2}}\left[\frac{1}{16}F^2_{2,0}\left(\cos\theta - 3\right) + \frac{1}{4}\cos^2\frac{\theta}{2}\left(4F'_{1,0}Z + F_{2,0}Z + Z^2\cos\theta - \frac{3}{2}Z^2\right)\right]$$

$$\left(\frac{\mathrm{d}\sigma}{\mathrm{d}\cos\theta}\right)^{s=1}_{\mathrm{NNLO}} = -\frac{4\pi\alpha^2}{M^2\sin^2\frac{\theta}{2}}\left[\frac{1}{24}F^2_{2,0}\left(\cos\theta - 3\right) + \frac{1}{4}\cos^2\frac{\theta}{2}\left(4F'_{1,0}Z - \frac{2}{3}F_{1,1}Z + \frac{2}{3}F_{2,0}Z + Z^2\cos\theta - \frac{5}{3}Z^2\right)\right]$$

$$\left(\frac{\mathrm{d}\sigma}{\mathrm{d}\cos\theta}\right)^{s=\frac{3}{2}}_{\mathrm{NNLO}} = -\frac{4\pi\alpha^2}{M^2\sin^2\frac{\theta}{2}}\left[\frac{5}{144}F^2_{2,0}\left(\cos\theta - 3\right) + \frac{1}{4}\cos^2\frac{\theta}{2}\left(4F'_{1,0}Z - \frac{2}{3}F_{1,1}Z + F_{2,0}Z + Z^2\cos\theta - \frac{13}{6}Z^2\right)\right]$$

$$\left(\frac{\mathrm{d}\sigma}{\mathrm{d}\cos\theta}\right)^{s=2}_{\mathrm{NNLO}} = -\frac{4\pi\alpha^2}{M^2\sin^2\frac{\theta}{2}}\left[\frac{1}{32}F^2_{2,0}\left(\cos\theta - 3\right) + \frac{1}{4}\cos^2\frac{\theta}{2}\left(4F'_{1,0}Z - \frac{2}{3}F_{1,1}Z + \frac{2}{3}F_{2,0}Z + Z^2\cos\theta - \frac{7}{3}Z^2\right)\right]$$

Exhibit universal structures at first two orders. NNLO still bears some interesting spin-dependent patterns

Light non-relativistic spin-1/2 projectile

$$\left(\frac{\mathrm{d}\sigma}{\mathrm{d}\cos\theta}\right)^{s}_{(v^0)} = \frac{2\pi Z^2\alpha^2}{\mathbf{k}^4}\frac{m^2(M+m)^2\left(\sqrt{M^2-m^2\sin^2\theta}+m\cos\theta\right)^2}{M\sqrt{M^2-m^2\sin^2\theta}\left(M-\cos\theta\sqrt{M^2-m^2\sin^2\theta}+m\sin^2\theta\right)^2}$$

$$= \frac{8\pi Z^2\alpha^2 m^2}{\mathbf{k}^4\sin^4\frac{\theta}{2}} - \frac{\pi Z^2\alpha^2 m^4}{M^2\mathbf{k}^4} + \mathcal{O}\left(\frac{m^6}{M^4\mathbf{k}^4}\right).$$

$$\left(\frac{\mathrm{d}\sigma}{\mathrm{d}\cos\theta}\right)^{s}_{(v^2)} = \frac{\pi\alpha^2}{\mathbf{k}^2\sin^2\frac{\theta}{2}}\left[\frac{Z^2\cos^2\frac{\theta}{2}}{2\sin^2\frac{\theta}{2}} - \frac{Z^2 m\cos^2\frac{\theta}{2}}{M} - \frac{Zm^2}{4M^2}f^{s}_{\mathrm{NNLO}} + \mathcal{O}\left(\frac{1}{M^3}\right)\right]$$

$$f^{s=0}_{\mathrm{NNLO}} = 16F'_{1,0} + Z\cos\theta - Z,$$

$$f^{s=\frac{1}{2}}_{\mathrm{NNLO}} = 16F'_{1,0} + Z\cos\theta + 4F_{2,0} - 3Z,$$

$$f^{s=1}_{\mathrm{NNLO}} = 16F'_{1,0} + Z\cos\theta - \frac{8}{3}F_{1,1} + \frac{8}{3}F_{2,0} - \frac{11}{3}Z,$$

$$f^{s=\frac{3}{2}}_{\mathrm{NNLO}} = 16F'_{1,0} + Z\cos\theta - \frac{8}{3}F_{1,1} + 4F_{2,0} - \frac{17}{3}Z,$$

$$f^{s=2}_{\mathrm{NNLO}} = 16F'_{1,0} + Z\cos\theta - \frac{8}{3}F_{1,1} + \frac{8}{3}F_{2,0} - \frac{19}{3}Z.$$

Reproducing the soft behavior from HPET

$$\mathcal{L}_{\rm HPET} = \bar{h}_v \left(iD_0 + c_2 \frac{\mathbf{D}^2}{2M} + c_F e \frac{\boldsymbol{\sigma}\cdot\mathbf{B}}{2M} + c_D e \frac{[\boldsymbol{\nabla}\cdot\mathbf{E}]}{8M^2} + i c_S e \frac{\sigma\cdot(\mathbf{D}\times\mathbf{E} - \mathbf{E}\times\mathbf{D})}{8M^2} \right) h_v + \mathcal{O}(1/M^3)$$

HPET description of massless spin-1/2 projectile hitting spin-1/2 composite target:

$$\begin{aligned}
\mathcal{M}_{\rm HPET} &= -\sqrt{1 + c_2 \frac{\mathbf{p}'^2}{2M^2}} \frac{e^2}{q^2} \Bigg\{ - Z \bar{u}_{\rm NR} u_{\rm NR} \bar{u}(k') \gamma^0 u(k) + \frac{c_2 Z}{2M} \bar{u}_{\rm NR} u_{\rm NR} \bar{u}(k') \mathbf{p}'\cdot\boldsymbol{\gamma} u(k) \\
&\quad - \frac{c_F}{4M} \bar{u}_{\rm NR} \left[\not{q}, \gamma^\mu \right] u_{\rm NR} \bar{u}(k') \gamma_\mu u(k) - \frac{c_D q^2}{8M^2} \bar{u}_{\rm NR} u_{\rm NR} \bar{u}(k') \gamma^0 u(k) \Bigg\} \\
&= \frac{e^2}{q^2} \Bigg\{ Z \bar{u}_{\rm NR} u_{\rm NR} \bar{u}(k') \gamma^0 u(k) + \frac{c_F}{4M} \bar{u}_{\rm NR} \left[\not{q}, \gamma^\mu \right] u_{\rm NR} \bar{u}(k') \gamma_\mu u(k) + \frac{c_D q^2}{8M^2} \bar{u}_{\rm NR} u_{\rm NR} \bar{u}(k') \gamma^0 u(k) \Bigg\}
\end{aligned}$$

$$\begin{aligned}
\left. \frac{\mathrm{d}\sigma}{\mathrm{d}\cos\theta} \right|_{\rm EFT} &= \frac{\pi\alpha^2 Z^2 \cos^2\frac{\theta}{2}}{2\mathbf{k}^2 \sin^4\frac{\theta}{2}} - \frac{\pi\alpha^2 Z^2 \cos^2\frac{\theta}{2}}{M|\mathbf{k}|\sin^2\frac{\theta}{2}} \\
&\quad - \frac{\pi\alpha^2}{8M^2 \sin^2\frac{\theta}{2}} \left[Z^2 (\cos 2\theta - 1) + c_D Z (\cos\theta + 1) + c_F^2 (\cos\theta - 3) \right]
\end{aligned}$$

$$\begin{aligned}
c_F &= F_{2,0}, \\
c_D &= 2F_{2,0} + 8F'_{1,0} - F_{1,0},
\end{aligned}$$

Reproducing the soft behavior from NRQED+HPET

$$\mathcal{L}_{\rm NRQED} = \psi^\dagger \left[iD^0 + d_2 \frac{\mathbf{D}^2}{2m} + d_4 \frac{\mathbf{D}^4}{8m^3} + d_F e \frac{\boldsymbol{\sigma}\cdot\mathbf{B}}{2m} + d_D e \frac{[\boldsymbol{\nabla}\cdot\mathbf{E}]}{8m^2} + i d_S e \frac{\boldsymbol{\sigma}\cdot(\mathbf{D}\times\mathbf{E} - \mathbf{E}\times\mathbf{D})}{8m^2} \right] \psi$$

NRQED+HPET description of slowly-moving spin-1/2 projectile hitting a static spin-1/2 composite target

$$\begin{aligned}\mathcal{M}_{\rm EFT} =& \frac{e^2}{\mathbf{q}^2}\left[-Z + \frac{(c_D - 2c_2 Z)\,\mathbf{p}'^2}{8M^2}\right]\xi^\dagger \left[1 + \frac{d_2}{4m^2}\left(\mathbf{k}^2 + \mathbf{k}'^2\right) - \frac{d_D}{8m^2}|\mathbf{k}'-\mathbf{k}|^2 - \frac{i d_S}{4m^2}\boldsymbol{\sigma}\cdot(\mathbf{k}\times\mathbf{k}')\right]\xi \bar{u}^{\lambda'}_{\rm NR} u^{\lambda}_{\rm NR} \\ & - \frac{c_F e^2}{4M\mathbf{q}^2}\xi^\dagger \left\{ (k^i + k'^i)\left[\frac{d_2}{2m} + \frac{d_2^2 - d_4}{8m^3}(\mathbf{k}^2 + \mathbf{k}'^2)\right] + \frac{i d_F}{2m}\left[\boldsymbol{\sigma}\times(\mathbf{k}'-\mathbf{k})\right]^i - \frac{i d_S}{16m^3}(\mathbf{k}'^2 - \mathbf{k}^2)\left[\boldsymbol{\sigma}\times(\mathbf{k}'-\mathbf{k})\right]^i \right\}\xi \\ & \times \bar{u}^{\lambda'}_{\rm NR}\left[\gamma^i, \boldsymbol{\gamma}\cdot\mathbf{q}\right] u^{\lambda}_{\rm NR}. \end{aligned} \tag{19}$$

$$\begin{aligned}\left.\frac{d\sigma}{d\cos\theta}\right|_{\rm EFT} =& \frac{\pi\alpha^2 m^2 Z^2}{2\mathbf{k}^4 \sin^4\frac{\theta}{2}} - \frac{\pi\alpha^2 m^4 Z^2}{M^2\mathbf{k}^4} + \frac{\pi\alpha^2 Z}{2\mathbf{k}^2\sin^2\frac{\theta}{2}}\left\{ \frac{Z\,(d_D\cos\theta - d_D + 2)}{2\sin^2\frac{\theta}{2}} \right. \\ & \left. - \frac{m}{M}(d_D\cos\theta - d_D + 2) - \frac{m^2}{2M^2}\left[Z(2 + d_D - 4c_2) + Z\cos\theta(2 - d_D) + 2c_D\right]\right\}\end{aligned}$$

$d_2 = d_4 = d_F = d_D = d_S = 1$

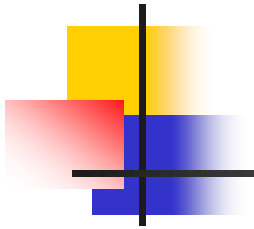

Thanks!